Modeling, Simulation and Development of Supervision Control System for Hybrid Wind Diesel System

By

Vigneshwaran Rajasekaran

A Thesis Submitted to Saint Mary's University, Halifax, Nova Scotia
in Partial Fulfillment of the Requirements for
the Degree of Master of Science in Applied Science

July 19, 2013, Halifax, Nova Scotia

Copyright Vigneshwaran Rajasekaran, 2013

Approved: Dr. Adel Merabet
Supervisor
Division of Engineering

Approved: Dr. Hussein Ibrahim
Co-Supervisor
Wind Energy TechnoCentre
Gaspe, Quebec

Approved: Dr. Alain Joseph
External Examiner
Applied Energy Research Lab
N.S. Community College –
Waterfront Campus

Approved: Dr. David Swingler
Supervisory Committee Member
Division of Engineering

Approved: Dr. Kevin Vessey
Dean of Graduate Studies

Date: July 19th, 2013

Modeling, Simulation and Development of Supervision Control System for Hybrid Wind Diesel System

by Vigneshwaran Rajasekaran

Abstract

A simulation-based research work on developing supervision control system for hybrid wind diesel system (HWDS) is presented. Simulation models of HWDS based stand-alone system and micro-grid systems are developed with different types of generators for a fully-rated converter based wind energy conversion system (WECS). A multi-variable control system is developed and implemented into the simulation models of HWDS. An appropriate control system is developed for each generator chosen for the WECS in the HWDS. This control system optimizes the power generation and ensures power sharing between the two sources. A control system for load voltage regulation and power system frequency regulation is developed and implemented to maintain the power quality at optimum level. An improved maximum power point tracking control scheme is simulated to achieve maximum power generation from the available wind. Also a governor control system is simulated for the diesel generation system. In this work, HWDS based stand-alone system and micro-grid system is simulated to study the performance of the developed control system. The complete HWDS is modeled and simulated in a MATLAB Simulink environment. Simulation results to validate the performance of the developed control system are presented.

July 19th, 2013

ACKNOWLEDGEMENT

I would like to extend my gratitude to all those who helped me to successfully complete my thesis project. First, I would like to thank Saint Mary's University for providing me the opportunity to pursue the MSc Applied Science program with funding. I am grateful to my project supervisor, Dr. Adel Merabet, for his help, guidance and financial support throughout my program of study. I am thankful for the support provided by Dr. Hussein Ibrahim and Wind Energy TechnoCentre, Quebec.

I would like to thank all the members of the supervisory committee and the external examiner for their valuable comments and suggestions provided for my thesis. Without their guidance and feedback, the thesis work could not have been a success. I would also like to thank the entire research group of Laboratory of Control Systems and Mechatronics (LCSM), Division of Engineering at Saint Mary's University for their support and help. And I would also like to thank all the University officials who directly or indirectly helped me throughout my program of study.

Finally, I express my gratitude to my parents for their constant support and encouragement throughout my years of study. This accomplishment would not have been possible without them.

July 19th, 2013

Table of Contents

List of Figures

List of Abbreviations

AC	Alternating current
CanWEA	Canadian Wind Energy Association
DC	Direct Current
DFIG	Doubly Fed Induction Generator
DG	Diesel Generation
d-q	Direct and Quadrature axis
GTO	Gate turn-off
HWDS	Hybrid Wind Diesel System
IEEE	Institute of Electrical and Electronics Engineers
IG	Induction Generator
IM	Induction Machine
IGBT	Insulated Gate Bi-polar Junction Transistor
KVA	Kilo Volt Ampere
KW	Kilo Watts
MW	Mega Watts
PI	Proportional-integral
PID	Proportional-integral-derivative
PLL	Phase-locked-loop
PMSG	Permanent Magnet Synchronous Generator
PWM	Pulse Width Modulation
SCIG	Squirrel-cage induction generator
SG	Synchronous generator
STATCOM	Static synchronous compensator
TCE	TechnoCentre Éolien
WECS	Wind Energy Conversion System
VSC	Voltage source converter
WO	Wind-only mode
WD	Wind-Diesel mode
WRIG	Wound-rotor induction generator
WTG	Wind Turbine Generation

Nomenclature

Induction Machine

s	Stator quantity
r	Rotor quantity
ls	Leakage-stator
lr	Leakage-rotor
d	d-axis parameter
q	q-axis parameter
ω_m	Mechanical rotor angular velocity
Θ_m	Mechanical rotor angular position
ω_r	electrical angular velocity
T_{em}	Electromagnetic torque
T_m	Mechanical shaft torque
J,H	combined rotor-load inertia coefficient and inertia respectively
F	combined rotor-load viscous friction
Lm	Magnetizing inductance
L_S	Total stator inductance
L'_r	Total rotor inductance

DFIG-Rotor Side Converter Control System Parameters

ω_{ref}	reference rotor speed
T_{ref}	reference torque
ω_{error}	Angular speed error
K_{p_torque}	Proportional gain of torque controller
K_{i_torque}	Integral gain of torque controller
I_{dr_ref}	d-axis reference current

I_{dr_error}	d-axis current error
I_{qr_ref}	q-axis reference current
I_{qr_error}	q-axis current error
V^*_d	d-axis reference voltage
V^*_q	q-axis reference voltage
$V_{rotor\_control}$	Control voltage for PWM generator

DFIG-Grid Side Converter Control System Parameters

V_{dc}	dc-link voltage
V_{dc_ref}	reference dc-link voltage
V_{dc_error}	dc-link voltage error
I_{d_ref},	d-axis reference components of the grid current
I_{q_ref}	q-axis reference components of the grid current
K_{p_Vdc}	proportional gain of voltage regulator
K_{i_Vdc}	integral gain of voltage regulator
$K_{p\_gc\_CR}$	proportional gain of current regulator
$K_{i\_gc\_CR}$	Integral gain of current regulator
I_{abc_gc}	Three phase grid current
L_{Grid}	Grid side coupling inductance
R_{Grid}	Grid side coupling resistance
$V_{grid\_control}$	Control voltage for PWM generator

Permanent Magnet Synchronous Generator (PMSG)

q	q-axis parameter
d	d-axis parameter
v	Voltage
ω_r	Rotor angular velocity

ϕ	Flux induced by permanent magnets
P	Number of pole pairs
T_e	Electromagnetic Torque
J	Combined rotor-load inertia
F	Combined rotor-load viscous friction
T_m	Mechanical shaft torque
Θ	Mechanical rotor angular position
T_f	Static friction torque in shaft
R_S	Resistance of stator windings

PMSG-Machine side Converter Control System Parameters

ω_{ref}	reference rotor speed
T_{ref}	reference torque
ω_{error}	Angular speed error
K_{p_torque}	Proportional gain of torque controller
K_{i_torque}	Integral gain of torque controller
I_d^*	d-axis reference current
I_q^*	q-axis reference current
I_{abc}^*	Three phase stator reference current
I_{abc}	Three phase stator current

PMSG-Load side Converter Control System Parameters

V_{dc}	dc-link voltage
V_{dc_ref}	reference dc-link voltage
V_{dc_error}	dc-link voltage error
I_{d_ref}	d-axis reference current
I_{q_ref}	q-axis reference current
K_{p_Vdc}	proportional gain of voltage regulator
K_{i_Vdc}	integral gain of voltage regulator

K_{p_CR}	proportional gain of current regulator
K_{i_CR}	Integral gain of current regulator
I_{abc_gc}	Three phase grid current
I_{d_error}	d-axis current error
I_{q_error}	q-axis current error
I_{abc_load}	Three phase load current

Synchronous Machine

i_{kd}	Damper winding current
i_{fd}	Field current
ϕ_{mq}	q-axis Mutual flux
ϕ_{md}	d-axis Mutual flux
Vq	q-axis stator voltage
Vd	d-axis stator voltage
ω_R	Mechanical rotor speed
T_e	Electromagnetic torque
H	Inertia constant
T_m	mechanical torque
K_d	Damping factor
ω_0	speed of operation
R_S	stator resistance
L_{ls}	stator leakage inductance
L_{md}	d-axis magnetizing inductance
L_{mq}	q-axis magnetizing inductance
R'_f	field resistance
L'_{lfd}	field leakage inductance
R'_{kd}	d-axis damper resistance
R'_{kq}	q-axis damper resistance

L'_{lkd}	d-axis damper leakage inductance
L'_{lkq1}	q-axis damper leakage inductance
L'_{lkq2}	q-axis damper leakage inductance
J	inertial coefficient
P	number of pole pairs
T_f	friction torque
φ'_{fd}	field winding d-axis flux
φ'_{kd}	damper winding d-axis flux
φ'_{kq1}	damper winding q-axis flux
φ'_{kq2}	damper winding q-axis flux

Two-level Voltage Source Converter

v_{aN}	Phase-a voltage of two-level voltage source converter
m_a	amplitude modulation ratio
V_{dc}	DC-link voltage
$V_{carrier}$	peak voltage of carrier
V_m	peak voltage of modulating signal
V_{LL}	line-to-line output voltage

Chapter 1

Introduction

1.1. Background

Modernization of energy systems has been underway worldwide to improve the reliability in managing production and consumption of energy. Integration of renewable energy systems is also a significant part of this modernization for a sustainable future. In Canada there are 292 off-grid communities including 200 in Nordic climates, these communities have significant wind potential [1]. An estimated total population of approximately 200,000 people in these communities is not connected to the North American electrical grid [2]**.** Most of these communities utilize diesel generators for day-to-day electrical power needs. As diesel generators are a highly expensive option and contribute to carbon emission [3]**,** an alternative energy solution is required to reduce diesel consumption. Integrating and operating renewable energy systems in parallel as hybrid energy system can be a more reliable option. Researchers around the world are working to address the challenges concerning the operation of hybrid systems.

TechnoCentre Éolien (TCE) [4] located in Quebec has implemented research infrastructure to optimize hybrid wind-diesel system (HWDS) for the Nordic off-grid communities. TCE has made initiatives to build a micro-grid and use it as a tool for

research and development on smart energy systems. The current infrastructure consists of a wind turbine generation system, a diesel generation system, and compressed air storage units.

The idea of integrating a diesel generator (DG) unit with a wind turbine generation (WTG) system was initiated in the 1970's as a solution to overcome oil crisis and much research has been conducted throughout the world. At the same time wind power generation has gained popularity and is estimated to produce 12% of world's electricity requirement by 2020 [5]**;** hence hybrid wind diesel system (HWDS) is an economic reality to reduce the dependency on diesel.

The key benefits of opting for HWDS includes: a) a reduction in diesel consumption, b) a reduction in carbon emission, and c) a reduction in cost of operation. When incorporating renewable energy based generation into a large power system, the portion of power demand that will be generated from the renewable source are determined and used for deciding the major components of HWDS. The ratio of wind turbine annual energy output to annual primary energy demand is known as penetration level [6].

Based on the penetration level, the HWDS has three different schemes [6], which characterize the system's complexity: a) low penetration (20% penetration level) b) medium penetration (20 to 50% penetration level), and c) high penetration –where diesel generators are shut-down during high wind speeds. Higher saving of diesel fuel is achieved in the high penetration (HP) HWDS. HWDS is considered as economical

solution for supplying the weak-grids or isolated power systems. In comparison to large regular utility grids, operating an autonomous HWDS in an isolated power system is considered more challenging in regard to regulation of voltage and power system frequency under safe values [7]. HWDS with different penetration levels are discussed in chapter 5.

1.2. Literature Review

A HWDS is a hybrid combination of a WTG system and DG unit to supply the maximum portion of the load requirements from the wind resource, while supplying quality electrical power [8] i.e. electrical power supply with regulated frequency and voltage conforming to standard codes. However, a complex control system design is involved in ensuring the proper power sharing between WTG system and controllable DG unit to meet the power demand.

Several research projects have focussed on simulation and development of control systems for HWDS. The interaction between variable speed WTG system and DG units has been studied in [9]. The transition between diesel-only (DO) to wind-diesel (WD) mode has been simulated with several perturbations on HWDS, where the WTG system is connected to an isolated grid powered by a DG unit [10]. The transition from WD to wind-only (WO) mode is simulated, and transition from WO to WD mode is simulated in [11] [12] and [13]. A dynamic model of wind-diesel system with control system is developed to emulate the behaviour of hybrid system under situations like: a) fluctuating

wind speeds, b) wind gust and c) changing loads [14]. However in this work the multi-variable control approach to regulate speed for maximum power extraction and voltage regulation for power quality is not studied; this approach is required to optimize the performance of the system.

Disconnection of WTG system showing the transition from WD to DO mode is simulated for an isolated power system in [15]. A methodology to stabilize the voltage and frequency has been implemented by controlling the excitation of synchronous generator and governor of DG unit respectively [16]. A similar methodology has been simulated in [17]. Since the DG unit has been used for stabilizing both the voltage and frequency, it is under operation all the time. This means no reduction in diesel fuel consumption and operation of DG unit under all loading conditions. Under lower load condition the DG unit still consumes 40% of rated fuel consumption [18], leading to deterioration in performance.

A multi-level control strategy for stand-alone wind diesel system is simulated for providing high quality power output by regulating voltage and frequency in [19]. A power management for a wind-diesel system under different wind and load condition is discussed in [20]. Variable speed permanent magnet synchronous generator based wind turbine is simulated in [21] to show the control of active power supplied to low voltage micro-grids. The regulation of supply voltage and power system frequency for a hybrid wind-diesel-battery system supplying isolated load is investigated in [17]. In a similar work, a control strategy using dump loads and battery storage system is investigated for

standalone wind turbine operation [22]. Control systems based on fuzzy logic for hybrid system with wind and diesel power generation system is simulated in [23].

In some research works, simulation studies were conducted to establish hybrid system based micro-grids. A micro-grid based on a photovoltaic-wind-diesel hybrid system is modeled in [24] to show system behaviour under grid fault and islanded operation. A power control strategy for grid connected hybrid power generation system is studied in [25]. An MPPT control and control system for safe transient operation of grid-connected wind turbine is implemented in [26].

The dynamic behaviour of a system consisting of a wind farm and a diesel group is investigated for different perturbations in [27]. A dual mode linguistic hedge based fuzzy controller for a wind-diesel hybrid power system with a storage unit is simulated to compare the system performance with a PI and a conventional fuzzy controller in [28]. An extended fuzzy linear matrix equalities based system design for a hybrid wind-diesel-storage is proposed and studied in [29]. A frequency and power control strategy for an autonomous power system with a wind-diesel-storage system is developed and studied in [30]. A modified automatic voltage regulator based reactive power compensation for a hybrid wind diesel system is simulated and verified in [31]. The modeling of distributed control system for a wind diesel hybrid system with a battery based storage system is modeled and simulated in [32]. An intelligent controller based on neural network for a hybrid power system consisting of a solar, a wind and a diesel system is simulated in [33]. The power sharing and load voltage regulation for a medium penetration hybrid wind-diesel-storage based microgrid is investigated with a dynamic simulation model in [34].

Although the above discussed works cover the various aspects involved in the operation of HWDS, scientists and engineers still find a dearth of in-depth knowledge to commercialize technology in the areas such as: control systems for maximum power extraction from wind, HWDS based micro-grid operation and control systems focussed on improving power quality. In short, a multi-variable control approach for each individual power sources is yet to be addressed for HWDS application. The thesis work explores the possibility of developing a supervision control system with the multi-variable control approach. A maximum power point tracking scheme and a frequency regulation system for a hybrid wind diesel system is simulated in [35]; this work also includes the power sharing between the sources and sink. A control system for a hybrid wind-diesel based standalone power system is simulated in [36] for studying the system behaviour under change in operating mode from wind-diesel to wind-only mode; this work also discusses the power sharing. A dynamic model with a control system for hybrid wind-diesel based microgrid is simulated in [37] for understanding the system behaviour under islanded and grid-connected mode. The focus on control system for maximum power extraction and power quality improvement can significantly help in effective usage of WTG system and in turn reduce the diesel consumption along with the overall operating cost.

1.3. Objectives, Scope and Contribution of the Research Work

1) To develop simulation models for wind energy conversion system (WECS) and hybrid wind diesel system (HWDS) – For the simulation based study, simulation models of HWDS based stand-alone and micro-grid system, with different types of generator for WECS and appropriate control systems are studied.
2) To develop a control system for WECS to extract maximum power from wind in wind-only (WO) and wind-diesel (WD) mode of operation. Since wind is highly varying in nature, control systems are required to improve power generation performance and provide economical solution. Also there is a need to utilize the intermittent wind effectively. A maximum power point tracking (MPPT) control is implemented with the simulation models
3) To develop control systems for improving power quality of the generated power from HWDS. For any load whether domestic or industrial, the most basic criteria considered in supplying quality power are: regulated voltage and regulated system frequency. Since the operation of HWDS involves two sources of energy, the voltage and frequency of power supply tends to fluctuate and needs to be regulated for ensuring optimum quality in power supply. Voltage and frequency regulation systems are developed and implemented into the simulation models
4) To simulate the transition between WO and WD mode of operation in HWDS. Some of the reasons for operating HWDS in these two operating modes are to: 1) share the required power generation between wind turbine and diesel generator, 2) increase

reliability of power supply and 3) reduce usage of the diesel generator. Transition between the two modes is simulated for HWDS models

Contribution – A part of the research infrastructure at TCE focuses on integrating the wind turbine generation (WTG) system with diesel generation (DG) unit and control the power generation of both to supply test loads. For this, TCE requires to develop control systems for HWDS. The thesis project is envisaged to provide knowledge on technical feasibility of control systems development for optimization of power generated from HWDS, where a multi-variable control approach is chosen and simulation models are developed for HWDS. The main contribution of the research is presented in chapters 4, 5 and 6.

1.4. Outline of the Thesis

Chapter 2- Focuses on the wind energy conversion system (WECS) that includes a background with fundamentals of WECS and various configurations of WECS

Chapter 3-Focuses on the electrical power conversion interface, and mainly contain discussion on the different types of electrical generators and power converters used in WECS applications.

Chapter 4- Focuses on the development of control system for wind energy conversion system with different types of electrical generators. It also includes a discussion on stand-alone and grid-connected WECS.

Chapter 5- Focuses on the development of a control system for hybrid wind diesel system (HWDS). Starting with brief background on HWDS, the chapter discusses the modeling of diesel generation system and frequency regulation control system. Also includes discussion on the stand-alone HWDS and HWDS based micro-grid.

Chapter 6- Results obtained from simulation study are presented and discussed**,** followed by the thesis conclusion.

Chapter 2

Wind Energy Conversion System

2.1. Introduction

Wind energy conversion systems (WECS) play a major role in extracting power from the abundantly available source of wind. It typically consists of a wind turbine, mechanical gear system (optional drive train), electrical generator, and power electronic interface and control system components. The major function of WECS is to convert the kinetic energy from the wind to electrical energy and supply the electrical grid or the loads directly. In recent decades, wind energy has become the predominant viable source of renewable energy. Scientists and engineers have gained considerable experience in handling small to large capacity wind generation systems.

2.2. Brief History and Background

The world's first wind turbine for electric power generation was constructed in the late 19^{th} century. Charles F. Brush built the first automatically operated wind turbine in Cleveland in 1887 [38]**.** In the early 20^{th} century, wind turbine generation technology gained more attention and two major technical advancements were added between 1940

and 1950: a) DC generators were replaced by the AC generators and b) wind turbine structures with three blades were introduced.

In the 1970s, the capacity of wind turbine power generation system increased significantly to the hundred kW range. Then wind turbines with megawatt (MW) generation capacity were operated in 1980s, making a significant contribution to renewable energy generation sector. In the same year, wind powered distributed generation systems were initiated [39]. As wind power generation technology progressed, the cost factor was the major concern to handle. The late 1990s saw wind power emerging as a major addition in scope of renewable energy generation source and a significant sustainable source of energy.

Over the last decade, wind power generation has attracted attention of the general public and is considered to be the fastest growing renewable energy source. Much more rapid growth of global installation capacity is expected in next decade with favourable policies being instituted (or in process) throughout the world such as Renewable Portfolio Standard (RPS) [40]**.** These policies promote the increase of power production by placing obligation on electricity supply companies to produce a specified fraction of power from renewable energy sources during a period. Today wind energy has become topology specific, abundant, clean and potential source of alternative energy option suitable for large scale power generation.

The global installed capacity of wind power generation systems in 2004 was 39 giga watts (GW) with 30% growth rate annually [41]**.** Wind power generation is projected to

produce 12% of world's electricity requirement by 2020 [5]**.** As far as Canada is concerned, wind farms all together have a current capacity of 6578MW – enough to power over 2 million homes or equivalent to about 3% of Canada's total electricity demand. Canada's wind resource is well distributed in rural areas throughout the country with various wind farms in operation, and more now under construction [42]**.** The Canadian Wind Energy Association (CanWEA) believes that wind energy can support 20 percent of Canada's electricity demand by 2025 by adding 55,000 MW of clean generating capacity that will strengthen the electrical grids and head off potential power shortages (canWEA WindVision 2025 program) [42]**.**

2.3. Major Components of Wind Energy Conversion System

2.3.1. Wind Turbines

Wind turbines are machines employed for converting the kinetic energy of the wind into mechanical energy, where the wind energy generated depends primarily on the wind speed [43]. A wind turbine generation system consists of turbine blades, generator, rotor, nacelle (gearbox and generator drive), shaft, drive or coupling device, converter and control system.

2.3.2. Mechanical Gearbox

A gearbox is a mechanical interface between the turbine rotor and an electrical generator through planetary gears. The gearbox is responsible for matching the speed of the

generator with the speed of the turbine by a certain conversion factor. Gearboxes are mostly used for converting the speed between low speed shafts of turbine to high speed shaft of electrical generator. The usage of a gearbox is decided by the type of electrical generator to be integrated into wind energy conversion system. Figure 2.1 shows a cut-away view of a typical wind turbine system [44].

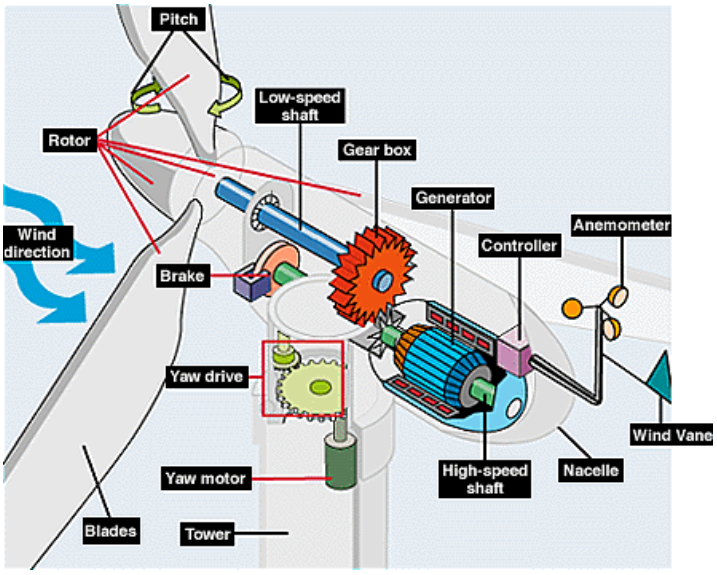

Fig.2. 1. Cut-away view of wind turbine system with major components [44]

2.3.3. Electrical Generator

The electrical generator is a machine that uses the mechanical torque from a prime mover (wind turbine rotor) and converts the mechanical energy to electrical energy. Depending on the type of electrical generator, the rotor shaft of the wind turbine is generally connected to the shaft of the generator either directly or through a mechanical gearbox. There are different types of generator used with wind turbine in a wind energy conversion

system. Most of the modern wind turbines are integrated with three phase AC generators [43].

2.3.4. Power Electronic Converters

Power electronic converters are electrical devices that process and control the flow of electrical energy by supplying optimal amount of current and voltage to suit the needs of any load, electrical power grid etc. [45].

In earlier times, power production based on wind energy had less impact on the electrical power system control, but in recent years the increased size of wind power production units tends to have impact on the stability of the power system operation. Initially the induction generator (IG) based wind turbine systems connected directly to electrical grid were the commonly used technology. This could cause damaging effects as the sharp fluctuation in the wind power gets transferred directly to the electrical grid. There were hardly any control system methods to handle active and reactive power in the wind power generation systems, which have greater significance in regulating voltage and frequency of the system. With increase in the power generation capacity of the wind turbines systems, the power electronic converters became a necessary interface between WTG units and the electrical power grid [46].

With rapid advancements in the field of power electronics, the voltage and current ratings of the semiconductor devices increased with the improved features like: less

power losses, lower prices per KVA and higher reliability. Thus, the power electronic converters became popular options for improving the quality of power supply and the performance of the wind power generation system.

2.4. Various Configurations of Wind Energy Conversion System

The structure of the WECS is aimed at transforming the kinetic energy from incoming wind into electrical energy in two steps. First the mechanical power is harvested by the wind turbine, and then the wind turbine rotor drives an electrical generator to produce electrical power. Over the years, a large number of architectures for wind turbines have been explored. The current versions of the commercially available designs predominantly feature: horizontal axis, three-blades and upwind operation for wind turbines.

The two main electrical components of the WECS include the generator and power electronic converter. A wide variety of WECS configurations are possible with different design choices and combination of the two electrical components [47]. A broad classification of WECS fall in these two categories: a) fixed speed WECS without power converter interface, b) variable speed WECS with reduced capacity power converter interface and fully-rated power converter interface.

2.4.1. Fixed-Speed Wind Energy Conversion System

Figure 2.2 shows a typical configuration of a fixed-speed WECS without a power converter interface, where generally a transformer is used to connect the generator to the electrical grid. For this type of WECS, a squirrel cage induction generator (SCIG) is preferred. The rotational speed of SCIG is determined through the grid frequency and the number of poles in stator winding. In order for the generator to deliver its rated power at corresponding rated wind speed; a gearbox is employed to match the speed difference between the generator and wind turbine rotor.

The SCIG based WECS requires reactive power for production of active power, the increased consumption of reactive power can lead to low full load power factor and a high inrush currents at the initial start. To limit this inrush current a soft-starter circuit is used at initial start of the fixed-speed WECS and this circuit is bypassed during normal operation. In order to compensate the reactive power drawn a three-phase capacitor bank is used.

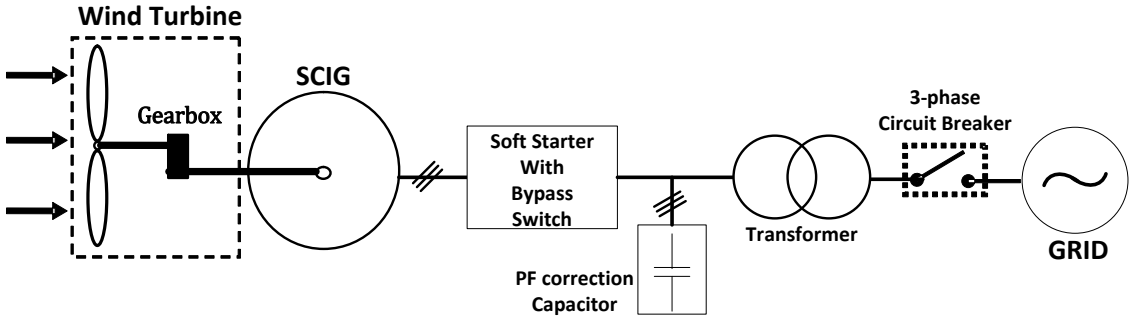

Fig.2. 2. Fixed-speed wind energy conversion system configuration

The fixed-speed WECS has the following advantages: mechanically simple, low maintenance and manufacturing cost, robust and stable. Their main drawbacks include: 1) rated power generation is possible only at a given wind speed, leading to a lower efficiency in energy conversion at other wind speeds and 2) with varying wind speed power delivered fluctuates, leading to stability and grid integration problems. Despite all these drawbacks, the fixed-speed WECS is still used in industry with rated capacity up to a couple of megawatts for each unit.

2.4.2. Variable-Speed Wind Energy Conversion System

The variable-speed WECS has several advantages over operation of fixed-speed WECS, which include: 1) reduced mechanical stress on wind turbine blades and structure, 2) reduced wear and tear of bearings and gearbox leading to reduced maintenance cost, 3) provides advantage of structural design for construction of larger wind turbine, 4) increased energy conversion efficiency and 5) increased operating life span of wind turbine. The main disadvantage of variable-speed WECS is the need of controlling the generator speed through the power converter interface, which increases the complexity and cost of the complete system. But the power converter facilitates the decoupling of generator from grid, enabling control over reactive power and active power on grid side [47]**.** Depending on the rated power of the power converter with respect to the total system operating power, the variable-speed WECS is classified into two types: a) WECS with reduced capacity power converter interface and b) WECS with fully-rated power converter interface.

2.4.2.1. Variable-Speed WECS with Reduced Capacity Power converter

For variable-speed WECS with reduced capacity power converter, a wound-rotor induction generator (WRIG) is preferred and commonly used [48]. Accessibility to control rotor currents without using the total power of the system makes it (i.e. WRIG) an ideal choice for variable-speed operation. The two main designs for WRIG configurations include: a) WRIG with power converter controlled variable resistance and b) double fed induction generator (DFIG) with four-quadrant power converter in rotor side.

A) WRIG with Rotor Resistance:

Figure 2.3 shows block diagram of a typical WRIG based WECS with a variable resistor connected to the rotor circuit. The variable-speed operation of turbine is achieved by changing the rotor resistance which in turn operates the generator at corresponding optimal torque/speed characteristics. Generally the rotor resistance is varied through the power converter. The range of adjustable speed is limited within 10% above the synchronous speed of the WRIG [49]**.** With this arrangement, the variable-speed operation maximizes the power captured from wind. Reactive power compensation and soft starter circuit are also required for this configuration.

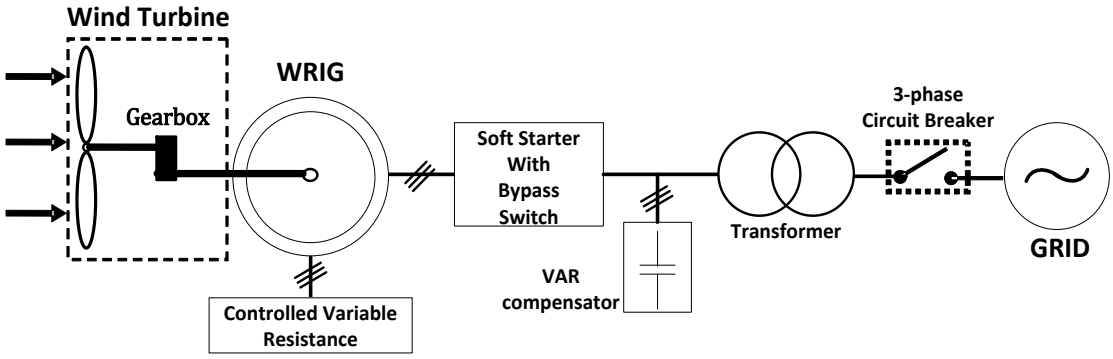

Fig.2. 3. Variable-speed WECS configuration with variable rotor resistance

B) Double Fed Induction Generator (DFIG) with Rotor Converter:

Figure 2.4 shows block diagram of a typical DFIG based WECS. This configuration is similar to the WRIG system discussed above with few modifications that include: a) replacement of variable resistor in the rotor side with a grid connected back-to-back power converters and b) removal of reactive power compensators or soft starter circuit. The power converters are used for adjusting the power factor of the system. The slip power being processed by these power converters is around 30% of the rated power of the generator. This reduces the cost of power converters compared to the WECS operated using full-rated power converters [47].

This configuration has many advantages that include: a) flexibility of bidirectional power flow in rotor circuit, b) extended operating speed range of the generator (±30%), c) increased power conversion efficiency of the complete system and d) improved dynamic performance compared to WRIG with variable resistor and fixed-speed WECS

configuration. DFIG based WECS is the most widely accepted and used configuration worldwide [50].

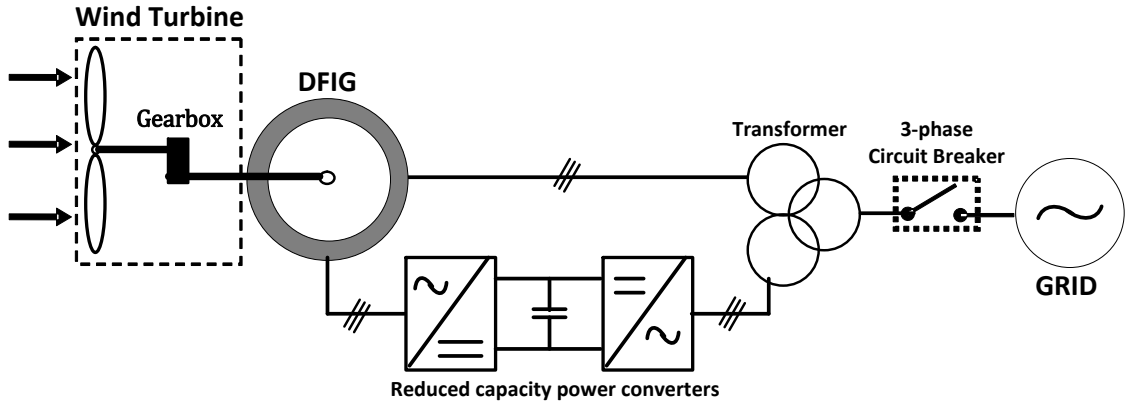

Fig.2. 4. Variable-speed WECS configuration with reduced capacity power converters

2.4.2.2. Variable-Speed WECS with Fully-Rated Power Converters

The overall performance of the variable-speed WECS is highly enhanced with the use of fully-rated power converter interface. Figure 2.5 shows the block diagram of this configuration. PMSG, SCIG and wound rotor synchronous generator with rated power of several megawatt ranges are majorly used (but not limited) in this configuration. The power converters are generally rated at the same power rating of the generator. The power converters in this configuration provide two main benefits: a) they allow the generator to be fully decoupled from the grid and operated at wide range of speeds and b) they enable control of reactive power between the grid and WECS. The increased complexity and cost of the system are the main drawback of this configuration.

This configuration enables operation of WECS without the use of a gearbox by using a synchronous generator with lower speed rating and large number of poles. Operation of WECS without gearbox has several advantages: a) it improves the efficiency of the system, b) reduces the initial cost and c) greatly reduces the maintenance cost. However, the cost of the generator and its installation increases due to lower speed rating leading to a larger diameter to accommodate large number of poles on its perimeter. Some of the possible power converters topologies used for this configuration are listed in table.1.

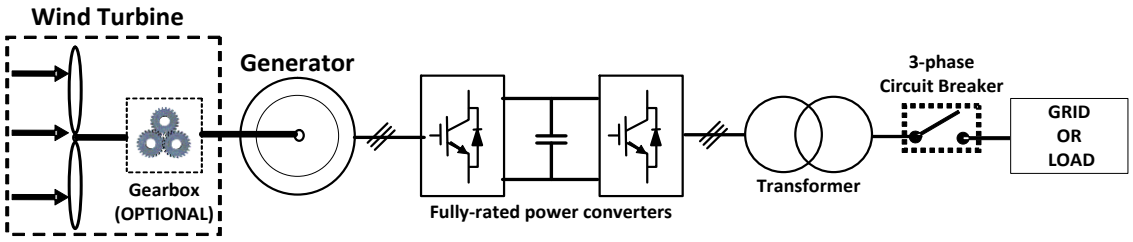

Fig.2. 5. Variable-speed WECS with fully-rated power converters

Table.1. Power Converter Topologies

Generator Side	Grid/load side
Diode bridge rectifier with DC-DC boost converter	Two level voltage source converter
Two level voltage source converter	Two level voltage source converter
Three-level neutral point clamped converter	Three-level neutral point clamped converter

Chapter 3

Electrical Power Conversion Interface

3.1. Introduction

In a WECS, the electrical power conversion interface mainly consists of electrical generator and power converters. With recent advancements in power conversion interface for wind turbines, various WECS configuration using variety of electrical generators [51] and power converter topologies were developed. The electrical generators and the power converter interface are discussed in detail in the following subsections.

3.2. Electrical Generator

The list of most commonly employed electrical generators for wind energy application (generally referred as wind generators) is shown in figure 3.1.

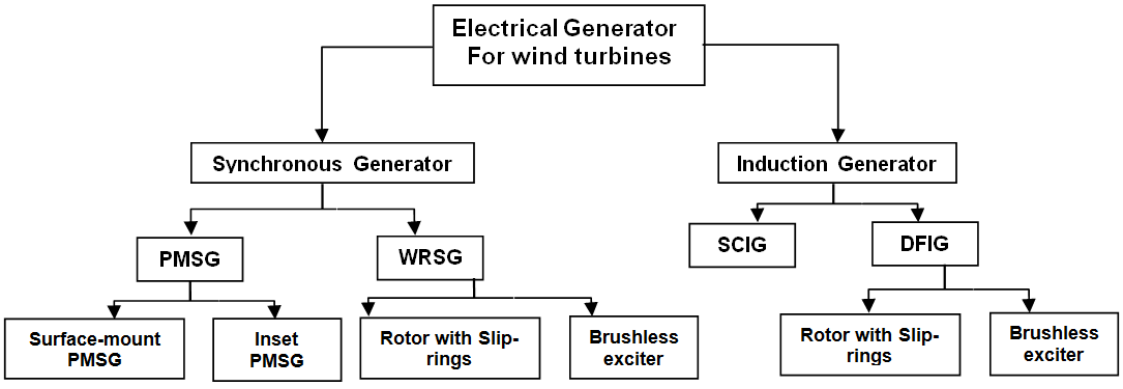

Fig.3. 1. Classification of electrical generators used in WECS

Based on the operating principle and physical construction; two prominent types of generator are commercially available: synchronous generator (SG) and induction generator. A wound-rotor type version of both the generator is available with the rotor being fed through slip rings and brushes or a brushless exciter embedded on the rotor shaft. The wound-rotor synchronous generator (WRSG) is mainly used in WECS where large number of poles is required and operating speed is low. The PMSG is one type that is commonly used in low speed operations. On the other hand the wound-rotor IG (also referred as DFIG) is the most widely accepted and used generator by wind turbine manufacturers and industries [52]**.** Different types of generator used in WECS are discussed in the sections below.

3.2.1. Induction Generator

An induction generator (also known as asynchronous generator) is an AC electromechanical machine that converts mechanical energy into electrical energy by operating under the principle of an electrical transformer. IG is a two-port system i.e. IG can be interfaced through two connection ports: 1) the electrical port in the form of AC terminals and 2) the mechanical port in the form of a rotating shaft. IG has the same physical construction and operates in same principle as that of an induction motor. An induction motor can be operated as IG by connecting the stator terminals to electrical system and driving the rotor shaft above its synchronous speed by a prime mover. The prime mover can be a wind turbine, an engine or anything that can supply required torque

to drive the motor above its synchronous speed. In this section the IG can be frequently referred as induction machine (IM).

Induction generators are preferred options in WECS because of several reasons: fine power generation capability under varying rotor speeds, does not require a separate dc-field excitation, ease of use with gearbox, simple, rugged and lighter in construction, less expensive, requires less maintenance, longer life-time and higher power production per unit mass. IGs can be employed both in grid-connected as well as in isolated WECS configuration. This allows IGs to be operated at constant or variable speed in a constant frequency system.

3.2.1.1. Construction of Induction Machine

A) Stator of Induction Machine

The stator core houses the three phase windings used in producing the rotating magnetic field. The stator core is built by stacking large number of stampings or laminations together. Laminations are insulated thin sheets (thickness ranging from 0.35 mm to 0.65 mm) made from high grade steel. Suitable slots for the windings are created on the stator core gap facing the inner periphery, it can be an open-slot, semi-closed slot or completely closed slot. The number of slots created is an integral multiple (3 times) of the number of stator poles in IM. Due to the constant change in polarity of the magnetic field within the stator core, occurrence of hysteresis and eddy-current loss is common. Hysteresis loss is

reduced by adding 3 to 5% of silicon to the high grade steel and eddy-current loss is reduced by using thin laminations.

B) Rotor of Induction Machine

There are two different types of rotor construction is available for induction machine: a) Squirrel-cage rotor used for SCIG and b) Wound rotor used for DFIG. Both rotors are built in the same way as that of stator discussed above, except the laminations are much thicker in this case.

Squirrel-cage rotor

In this type of rotor, a closed-type slot in a rectangular or circular shape is created on the core. The rotor shaft is placed in the centre and axially oriented to fit firmly by the key-way. The windings for a squirrel-cage machine consist of a series of metal bars. Depending on the power rating, these metal bars are constructed in different ways. For the low and medium power rated machines, molten aluminium is forced through the slots by pressure to form metal bars embedded directly into the slots. Then the metal bars are short-circuited by the end rings and cooling fan is fitted on the extension of end ring.

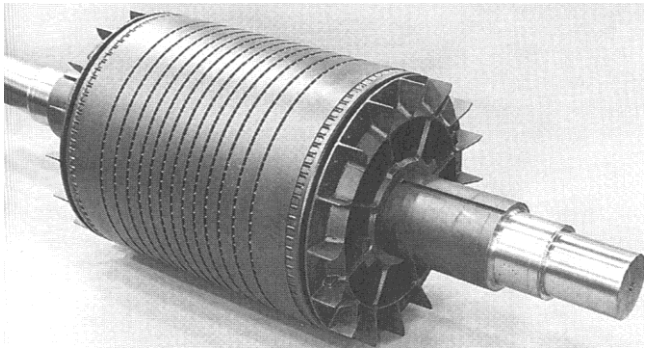

Fig.3. 2. Rotor of squirrel-cage induction machine [53]

As shown in figure 3.2, this type of rotor is simple and rugged in construction. For high power rated machines, off-the-shelf copper or brass bar is manually driven through the slots and the ends are silver-soldered or welded into end rings. The metal bars are generally inclined with respect to the shaft axis to reduce the magnetic humming within the machine and to mitigate the locking behaviour of the rotor.

Wound Rotor

This type of rotor houses a three-phase winding with equal number of poles as that in the stator. A typical wound rotor is shown in figure 3.3. These windings are generally star-connected whose terminals are made accessible by using slip-rings and brushes. This also gives a provision to include an external circuit for control systems in the rotor side.

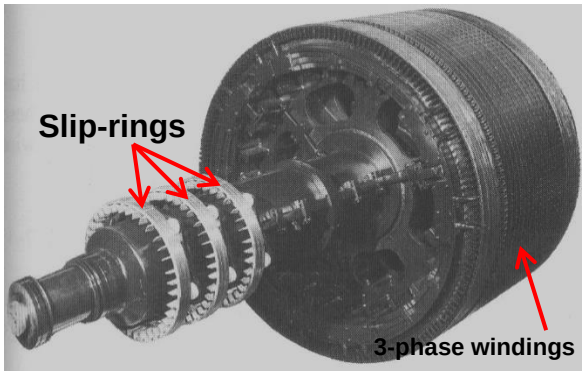

Fig.3. 3.Rotor of slip-ring or double-fed induction machine [53]

3.2.1.2. Induction Machine Model

The developed induction machine model is an equivalent of the physical system that is used for interfacing the wind turbine generation (WTG) system and the electrical power

grid network. The mechanical state variables for the rotor of the machine are included in the wind turbine model.

The electrical and mechanical systems are represented by state space models. An arbitrary dq-frame is used as reference for stator and rotor quantities. The electrical parameters and variables are referred to stator side; a prime symbol is used in the machine equations. Figure 3.4 and 3.5 shows the equivalent circuit model of electrical system in *q-axis* and *d-axis* frame of reference respectively.

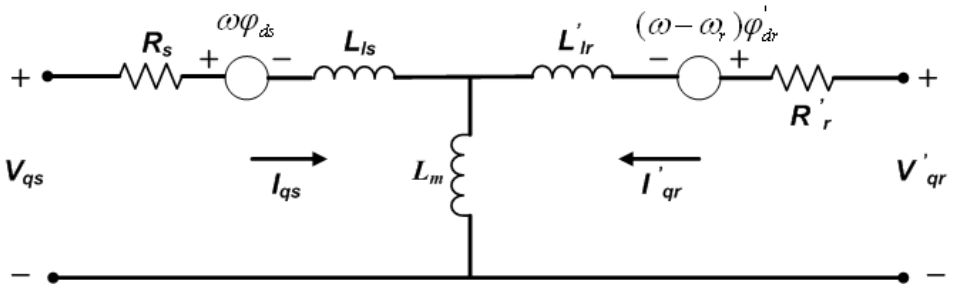

Fig.3. 4. Equivalent circuit model of electrical system of induction machine in q-axis frame [54]

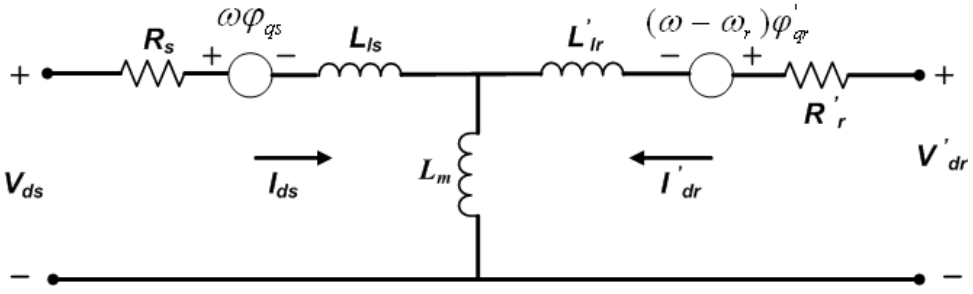

Fig.3. 5. Equivalent circuit model of electrical system of induction machine in d-axis frame [54]

The equations of electrical systems are given below [54]

$$V_{qs} = R_s i_{qs} + \frac{d}{dt}\varphi_{qs} + \omega\varphi_{ds} \tag{1}$$

$$V_{ds} = R_s i_{ds} + \frac{d}{dt}\varphi_{ds} - \omega\varphi_{qs} \tag{2}$$

$$V_{qr}^{'} = R_r^{'} i_{qr}^{'} + \frac{d}{dt}\varphi_{qr}^{'} + (\omega - \omega_r)\varphi_{dr}^{'} \tag{3}$$

$$V_{dr}^{'} = R_r^{'} i_{dr}^{'} + \frac{d}{dt}\varphi_{dr}^{'} - (\omega - \omega_r)\varphi_{qr}^{'} \tag{4}$$

Where,

$$\varphi_{qs} = L_s i_{qs} + L_m i_{qr}^{'} \tag{5}$$

$$\varphi_{ds} = L_s i_{ds} + L_m i_{dr}^{'} \tag{6}$$

$$\varphi_{qr}^{'} = L_r^{'} i_{qr}^{'} + L_m i_{qs} \tag{7}$$

$$\varphi_{dr}^{'} = L_r^{'} i_{dr}^{'} + L_m i_{ds} \tag{8}$$

$$L_s = L_{ls} + L_m \tag{9}$$

$$L_r^{'} = L_{lr}^{'} + L_m \tag{10}$$

The equations of the mechanical system are given below [54]

$$\frac{d}{dt}\omega_m = \frac{1}{2H}(T_{em} - F\omega_m - T_m) \tag{11}$$

$$\frac{d}{dt}\theta_m = \omega_m \tag{12}$$

The electromagnetic torque of the machine is calculated as per the below equation [54]:

$$T_e = 1.5(\varphi_{ds} i_{qs} - \varphi_{qs} i_{ds}) \tag{13}$$

The reactive power Q_S and active power P_S at the stator terminal is given below [55]:

$$P_S = V_{ds} i_{ds} + V_{qs} i_{qs} \tag{14}$$

$$Q_S = V_{qs} i_{ds} - V_{ds} i_{qs} \tag{15}$$

The reactive power Q_r and active power P_r at the rotor terminal is given below [55]:

$$P_r = V_{dr}^{'} i_{dr}^{'} + V_{qr}^{'} i_{qr}^{'} \tag{16}$$

$$Q_r = V_{qr}^{'} i_{dr}^{'} - V_{dr}^{'} i_{qr}^{'} \tag{17}$$

3.2.2. Permanent Magnet Synchronous Generator

Synchronous generators (SG) are extensively used in today's WECS with operating power range from kilowatts to few megawatts. SGs are majorly classified into two types: WRSG and PMSG. Both generators use different methods to produce rotor flux, rotor field windings are used in WRSG, whereas permanent magnets are used in PMSG.

The PMSGs are considered to be the promising option for the emerging direct driven (i.e. without gearbox) wind turbine applications [56]**.** Removal of gearbox can result in numerous benefits like: improved energy conversion efficiency, reduction in the weight of the wind turbine, no oil maintenance is required, precision associated with positioning is improved, reduced cost of power production, high torque density and higher overall efficiency is achieved. Operating at higher efficiency in low speed, high torque application can result in huge cost savings throughout the life span of the power drive. Also for a given mechanical specification, using PMSG in WECS results in: a) smaller

system size for rated efficiency and power factor and b) higher power density leading to maximum overall efficiency. Despite the higher initial cost, the attributes and benefits mentioned above makes PMSG an ideal choice for direct-driven WECS.

3.2.2.1. Construction of PMSG

Similar to the construction of induction generator, the PMSG has a stator and a rotor. A typical construction of PMSG is shown in figure 3.6. Since the stator construction is similar to that of the induction generator**,** section 3.2.1 can be referred. Usage of permanent magnets for flux production makes the PMSG a brushless machine; this highly reduces the maintenance cost. Due to the absence of rotor windings, achieving a higher power density is possible through reduced weight and size of the machine. With zero or negligible winding loss, the thermal stress on the rotor is highly reduced. The main drawback of PMSG is the usage of highly expensive permanent magnets that are prone to demagnetization. Based on the mounting of permanent magnets, the PMSG can be classified into two types: surface-mounted and inset PM generator.

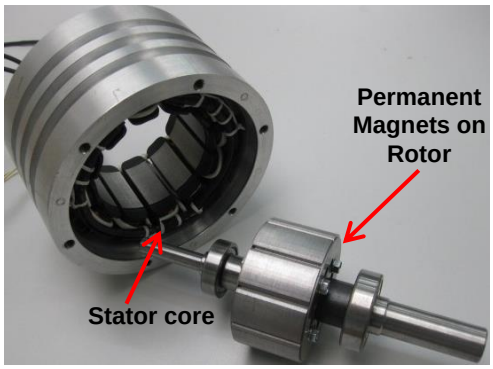

Fig.3. 6. Stator and Rotor of a PMSG (photo courtesy Technelec Ltd)

3.2.2.2. Permanent Magnet Synchronous Machine Model

The mechanical and electrical system of the machine is represented by state space model. In order to obtain sinusoidal electromotive force, the established stator flux by permanent magnets is also chosen as sinusoidal. Due to presence of a large air gap generally found in PMSG, it is assumed that the machine has a linear magnetic circuit and the core of either stator or rotor does not saturate. The equations of the electrical and mechanical system are given below. Equations (18) to (20) are used for electrical system and equations (21) and (22) are used for mechanical system [54].

$$\frac{di_d}{dt} = \frac{v_d}{L_d} - \frac{R_S i_d}{L_d} + \frac{L_q}{L_d} p\omega_r i_q \tag{18}$$

$$\frac{di_q}{dt} = \frac{v_q}{L_q} - \frac{R_S i_q}{L_q} - \frac{L_d}{L_q} p\omega_r i_d - \frac{\phi p\omega_r}{L_q} \tag{19}$$

$$T_e = 1.5p\left[\phi i_q + (L_d - L_q) i_d i_q\right] \tag{20}$$

$$\frac{d\omega_r}{dt} = \frac{1}{J}\left(T_e - T_f - F\omega_r - T_m\right) \tag{21}$$

$$\frac{d\theta}{dt} = \omega_r \tag{22}$$

3.3. Power Electronic Converter Interface

Power converters are used in a wide range of applications in WECS. In variable-speed WECS, they are mainly used for providing control access to torque and speed of the

machine. In fixed-speed WECS, they are used in reducing torque oscillation and high inrush currents during the start-up. A maximum power point tracking control system includes a power converter for operating the generator to track the optimum reference speed. This allows the wind turbine to be operated at optimum tip speed ratio and in turn achieve maximum power extraction from the wind. Also the power converters are employed to control active or reactive power and regulate voltage and frequency of power supplied to the grid or load. Depending upon the choice of the electrical generator and power ratings, several power converter configurations are possible for WECS. In this project, a pulse width modulation (PWM) controlled two-level three-phase voltage source converter with back-to-back connection is used in the simulation study.

The back-to-back converter (rectifier-inverter pair) is the predominantly used configuration for the variable speed WECS, consisting of PWM controlled voltage source converters (VSC) connected back-to-back. This configuration is a bidirectional power converter unit, where one converter works as rectifier and other converter operates as inverter throughout the power conversion process in either direction of power flow. A DC-link capacitor is connected in parallel between the two converters to achieve complete control over the current injected into the load or grid, the DC-link voltage across the capacitor is maintained at a higher magnitude than the load side line-to-line voltage.

3.3.1. Two-Level Voltage Source Converter

The two-level voltage source converter (VSC) consists of six switches, T1 to T6, with each switch connected to an anti-parallel free-wheeling diode as shown in figure 3.7. Depending on the operating power range, the choice of switch can be IGBT, MOSFET or IGCT etc. When the converter input is in the DC side to produce a three-phase variable voltage with variable frequency on AC side, then this converter is generally referred as an inverter and connected to AC loads. When the same converter input (with fixed magnitude and frequency) is on the AC side to produce variable DC voltage, it is often referred as rectifier and connected to DC loads. Thus the circuit of VSC allows bidirectional power flow.

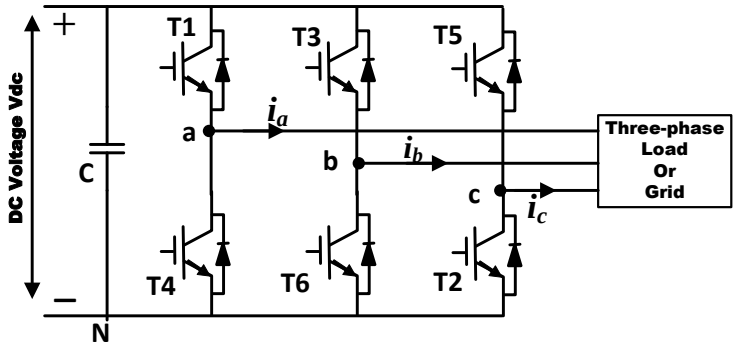

Fig.3. 7. Two-level voltage source converter

In figure 3.7, the converter output voltage in phase-a with respect to the point N in the DC bus i.e. phase voltage v_{aN} under linear modulation is given by the below expression [45].

$$v_{aN} = \frac{m_a V_{dc}}{2} \tag{23}$$

Where, m_a is the modulation index. The value of v_{aN} depends only on V_{dc} and state of the switch. Since one of the switches per leg is always ON at any given time, v_{aN} is independent of load current. In order to operate the VSC, a PWM scheme is used and this is discussed in the next section.

3.3.2. Pulse Width Modulation Scheme

The main objective of the PWM scheme is to provide control signals to the power converters and in turn control the magnitude and frequency of the output voltage supplied to the load or grid. A sinusoidal pulse width modulation (PWM) technique is used in this work.

Figure 3.8 shows the waveforms of sinusoidal PWM signal generated for operating a two-level three-phase VSC, where a saw-tooth wave represents the carrier signal and the three modulating signals are represented by $v_{a,}$ v_b and v_c. The amplitude modulation index m_a is used in controlling the fundamental frequency component of the converter output voltage and it is given by below equation [45].

$$m_a = \frac{V_m}{V_{carrier}} \tag{24}$$

Where $V_{carrier}$ and V_m are the peak voltage of carrier and modulating signal respectively.

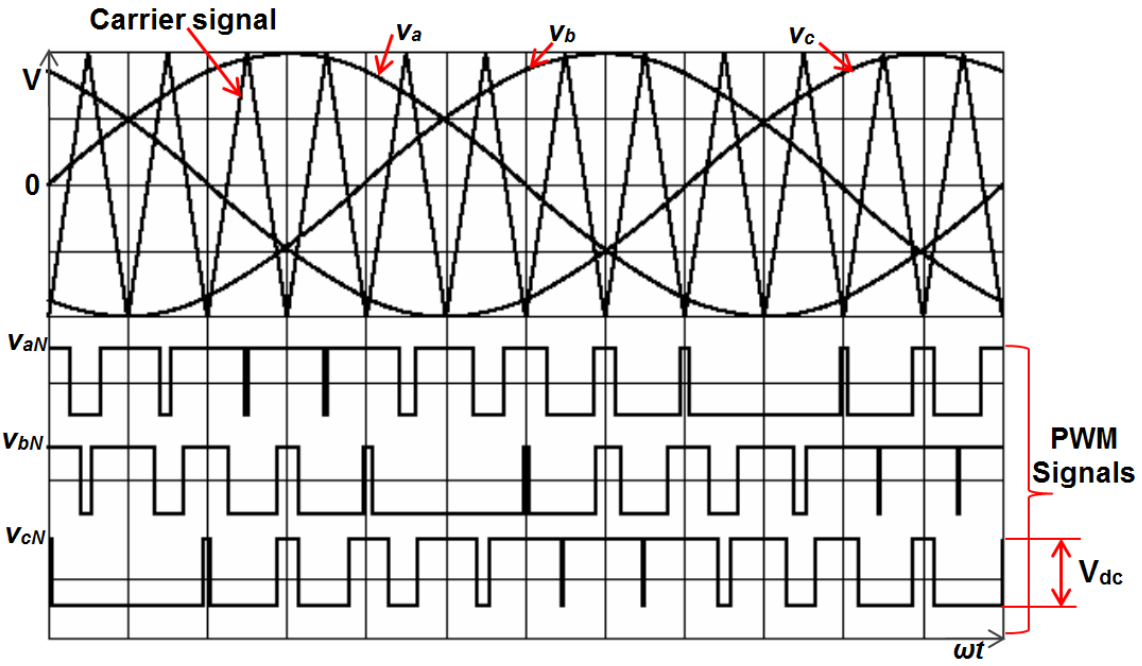

Fig.3. 8. PWM signal generation

The switching pulse for the switches T1 to T6, shown in figure 3.8, is generated by comparing the carrier signal and the modulating signal. Considering only one leg in the converter (in figure 3.7), when $v_a > V_{carrier}$, T1 is ON and T4 is OFF. During this period the converter terminal voltage i.e. the phase voltage with respect to negative DC bus is equal to V_{dc}. Similarly when $v_a < V_{carrier}$, T4 is ON and T1 is OFF, during this period the converter terminal voltage is zero. In order to avoid the occurrence of short circuit between the two switches in the same leg of the converter, a blanking time is introduced and both switches are maintained at OFF state during this time. Under linear modulation (i.e. m_a <1), the fundamental frequency component of the line-to-line output voltage V_{LL} of the converter is given by below equation [45].

$$V_{LL} = \frac{\sqrt{3}}{\sqrt{2}} v_{aN} = \frac{\sqrt{3}}{2\sqrt{2}} m_a V_{dc} = 0.612 m_a V_{dc} \quad (25)$$

Chapter 4

Control System for Wind Energy Conversion System

4.1. Introduction

Wind energy conversion systems (WECS) play a major role in extracting power from abundantly available source of wind. Since wind is varying in nature, it is very important to build control systems to handle the fluctuating power generation.

Wind turbine control systems are significant part of any modern WECS. These control systems ensure the efficient usage of the turbine capacity and increase the useful life of wind turbines by mitigating the impacts caused by aerodynamic and mechanical loads. With the increased capacity of individual turbine units, control systems for improving power quality are required to handle adverse effects on integration of WECS with the grid network. Using an active power control system reduces overall operating cost of WECS. Some of the primary control objectives include: a) power regulation – focussed on extracting the maximum power available from wind, b) improving power quality at the load end and c) aerodynamic stress mitigation for operation under safer mechanical limitation. Depending upon the choice of the generator and the power regulating system, the WECS has different configurations, as discussed in chapter 2.

4.2. General Control Methods for Wind Turbines

The recent decade has seen much advancement in WECS leading to the development of new control methods. Based on the speed of operation, WECS control methods can be broadly classified as: a) variable speed operation control and b) constant speed operation control.

A constant speed turbine system does not include any special control mechanism for controlling the shaft speed of the turbine, which makes it simple and less expensive option. Whereas a variable speed control provides better features like: less fluctuation in the power output, less mechanical stress on the wind turbine structure, provision for maximum power point tracking (MPPT) control to extract maximum possible energy from wind and reduced noise during low wind speeds.

Many research works concluded that the variable speed wind turbine system can produce higher capacity (20% more) of power than the constant speed turbine system, [57]**.** Different methods of control can be employed to limit or optimize power generation of WECS.

4.2.1. Modeling of Wind Turbine

The mechanical power output of the turbine is expressed as below [58].

$$P_m = C_p(\lambda, \beta)\frac{\rho A v_w^3}{2} \tag{26}$$

Where C_p is power coefficient of the turbine, ρ is the air density (kg/m^3), A is turbine swept area (m^2), V_w is wind speed (m/s), β is blade pitch angle (degree) and λ is tip speed ratio given by below equation [58].

$$\lambda = \frac{\omega_r R}{V_w} \tag{27}$$

Where ω_r is the rotor shaft speed and R is radius of the rotor blade. C_p of the wind turbine is function of β and λ; it is modelled using a generic expression [58] given by equation (28).

$$C_p(\lambda, \beta) = C_1\left(\frac{C_2}{\lambda_i} - C_3\beta - C_4\right)e^{\frac{-C_5}{\lambda_i}} + C_6\lambda \tag{28}$$

With

$$\frac{1}{\lambda_i} = \frac{1}{\lambda + 0.08\beta} - \frac{0.035}{\beta^3 + 1} \tag{29}$$

Equations (26) to (29) have been used in developing the mathematical model of wind turbine. Then for each WECS configuration discussed below, the parameters value are chosen from different wind turbine specifications (depending upon the generator power rating).

4.2.2. Maximum Power Point Tracking Control

In order to capture the maximum power at different wind speeds (mainly in below rated wind speed regime), the maximum power point tracking control method is employed. In

this method the shaft speed of the variable speed wind turbine is controlled to maintain an optimal tip speed ratio λ_{opt} and operate the system at maximum C_{p_max}, a typical characteristic curve is shown in figure 4.1.

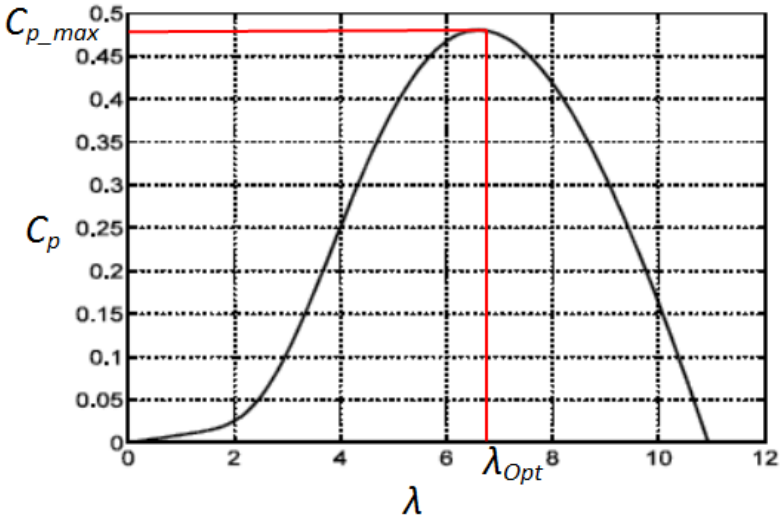

Fig.4. 1. Typical wind turbine characteristic with power coefficient verses tip speed ratio

By using the relations between speed, torque and mechanical power of a wind turbine, an optimal reference torque or speed can be calculated to control the generator and in turn achieve maximum power extraction. A variety of MPPT control schemes have been developed, three of these methods are discussed in consecutive subsections.

A) MPPT Using Data from Power Curve of Wind Turbine

Based on the wind turbine characteristic curve (power vs. wind speed) provided by the manufacturer, an MPPT control scheme can be developed. The manufacturer's curve gives an idea about the maximum power that can be generated by the turbine at various wind speeds, based on this, an MPPT profile is developed. A typical power characteristic curve of wind turbine is shown in figure 4.2.

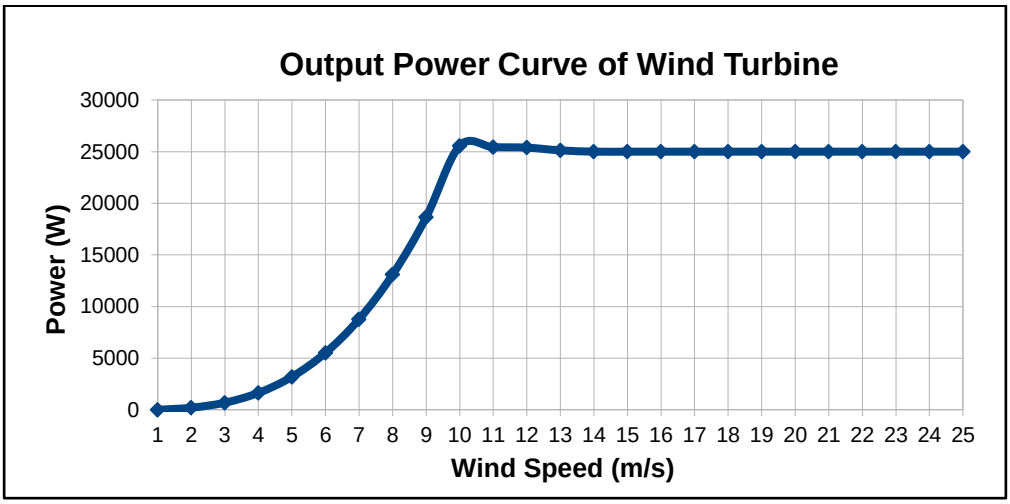

Fig.4. 2. Typical power characteristic of a wind turbine [59]

A series of power reference value corresponding to wind speed are generated online/offline using the profile. This reference power value is fed to the generator control system, which produces the required control signals for the generator side power converter. By controlling the power converters, the generator is controlled to track the reference power in such a way that the power generated is equal to reference power. Thus the maximum power extraction is achieved. In this analysis the power loss in the gearbox and drive train are not accounted.

B) MPPT Using Optimal Tip Speed Ratio

In order to operate the wind turbine at maximum power points, the tip speed ratio is maintained at an optimal value λ_{opt}. The control schematic for this method is shown in figure 4.3, where the reference speed ω_{ref} is generated from the wind speed measurement using value of the λ_{opt}. The power converters are controlled to vary the speed of generator rotor. The control system generates the fire pulse signals to control the power converters in such a way that the rotor speed ω_r follows the ω_{ref}. Thus the maximum power point tracking is achieved.

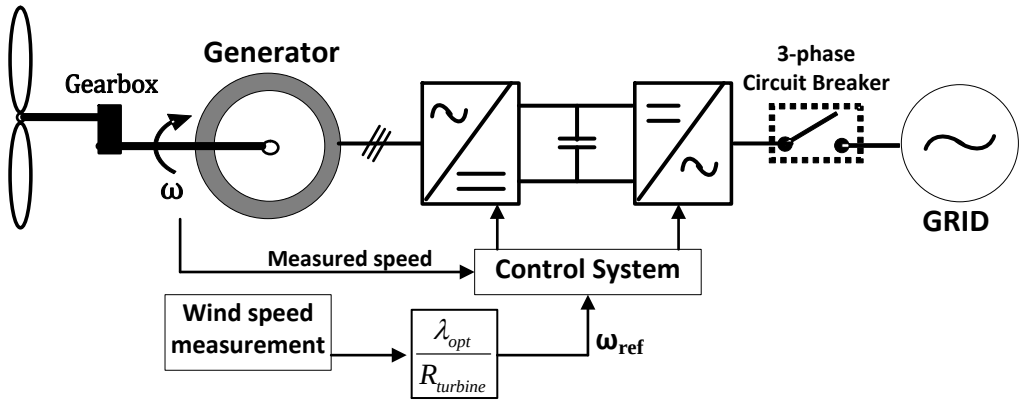

Fig.4. 3. WECS with optimal tip speed ratio based MPPT control scheme

C) MPPT Using Torque Controller

In this method the torque-speed relation is explored to develop an optimal control system, where the torque of the turbine T_m is a quadratic function of the generator rotor shaft speed ω given by below equation.

$$T_m \propto \omega_r^2 \tag{30}$$

Similar to the previous method the measured value of ω_r is used for calculating the desired reference torque T_m^* given by the below equation.

$$T_m^* = K_{opt}\omega_r^2 \tag{31}$$

Where K_{opt} is the optimal torque coefficient calculated from the specifications of the generator. Then the control system operates the generator to follow the reference torque T_m^* to achieve maximum power point tracking.

4.2.3. Improved MPPT Control Strategy

In this project an improved MPPT control strategy is used and implemented with the simulation model. In which a speed tracking system is developed to achieve maximum power extraction. For a wind turbine system, the power coefficient C_p represents the value of fraction of power converted into mechanical energy from the available wind energy. The C_p depends on the tip speed ratio λ (which in turn depends on turbine rotor shaft speed ω_r and wind speed V_w). Since C_p being function of λ, it reaches a maximum value for an optimum tip speed ratio $\lambda_{opt.}$ This value of C_p implies that the wind turbine is converting the maximum possible fraction of energy available in the wind into mechanical energy.

In order to operate the wind turbine with maximum C_p, the rotor shaft speed ω_r has to be controlled and regulated at an optimum value for which the wind turbine operates with tip-speed ratio λ_{opt}. Most of the common methods described above uses the wind

turbine characteristics to determine optimum tip speed ratio λ_{opt} and use equation (32) to calculate the reference speed for control system.

$$\omega_{ref} = \frac{\lambda_{opt} V_w}{R_{turbine}} \tag{32}$$

Since the common MPPT methods based on equation (28) requires the knowledge of wind turbine characteristics and wind speed measurements, it could affect the reliability of the control scheme with the presence of inaccuracies in the sensors and error in modeling of the wind turbine. In this work an MPPT control algorithm [60] developed based on power is simulated to determine the reference rotor speed ω_{ref}. A flowchart of the algorithm is shown in figure 4.4, where P_m mechanical power produced by the wind turbine.

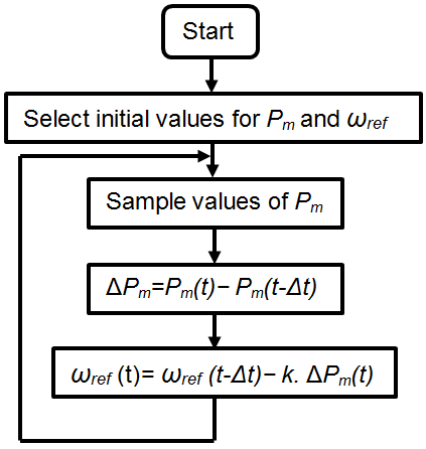

Fig.4. 4. Flowchart for the MPPT algorithm

For achieving continuous improvement in the speed tracking performance, the choice of the value of parameter k keeps changing with the change in wind speed. At low wind speed, the variation in the power generation is lower and vice versa at higher wind speed. Hence a large value of k is chosen at low wind speed and with increase in wind speed

value of *k* decreases. In similar methods [60] [61], the value of *k* is chosen manually from repeated simulations. In this work a new expression is proposed [62] to calculate *k* and it is expressed in equation (33).

$$k = \alpha.\omega_r(t)^{-1} \tag{33}$$

Where α is a positive gain. With this technique, the MPPT control system is improved and simulation results based are discussed in chapter 6.

4.3. Development of Control System

In this project, WECS based on three different machines has been modelled and implemented into simulation model. The machines used in the models are: squirrel-cage induction machine, double-fed induction machine and permanent magnet synchronous machine. Control system development for each of the three machines is detailed in following subsections.

4.3.1. PMSG Based WECS in Stand-Alone Power System

The modelling of the permanent magnet synchronous generator (PMSG) is discussed in section 3.2.2.2 of Chapter 3. The main objective of the developed control system is to control both power converters. The first converter is the machine side converter, where a vector control scheme is developed to provide torque control of the PMSG. The second converter is the load side converter, where a voltage regulator based on vector control

scheme is developed to provide load voltage regulation. The complete simulation model developed for the PMSG based wind energy conversion system is shown in figure 4.5.

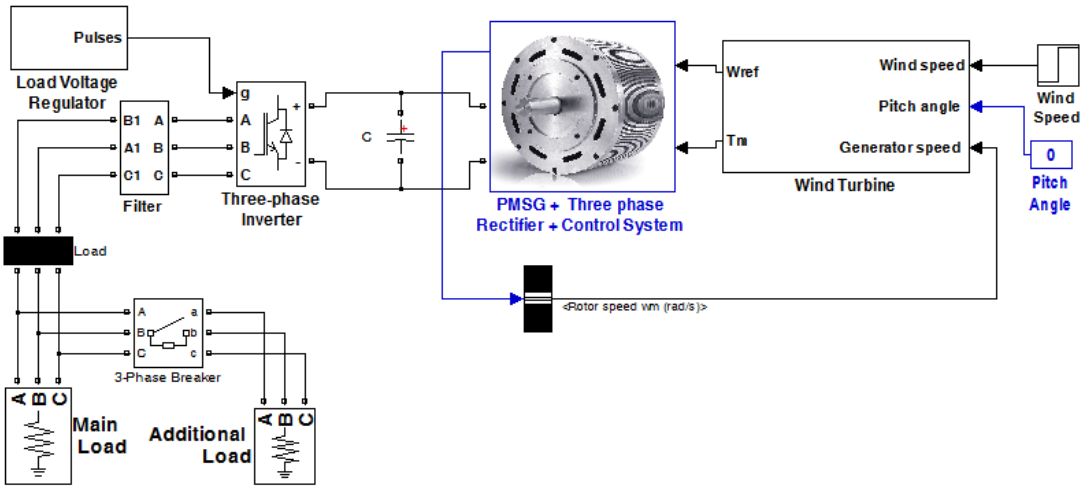

Fig.4. 5. Simulation model for PMSG based wind energy conversion system

A) Machine Side Converter Control System

A flux weakening vector control scheme is modelled for controlling the PMSG. The complete PMSG drive system consists of: three-phase power converter, generator, vector controller and speed controller. The developed control system model for the machine side converter is shown in figure 4.6.

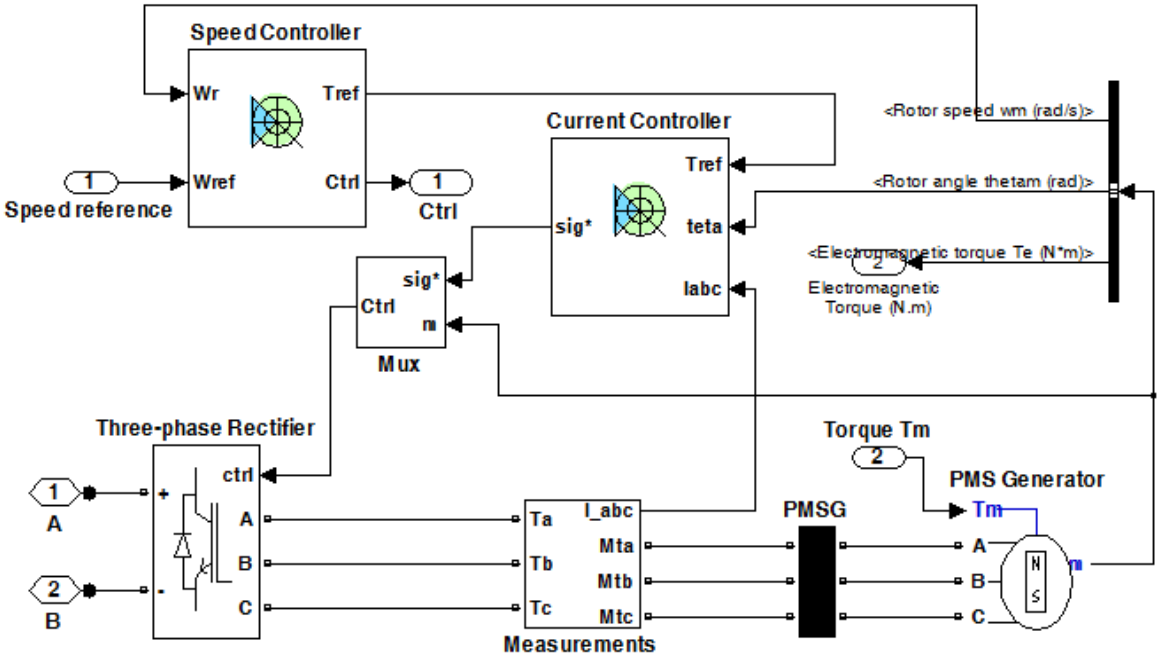

Fig.4. 6. Simulation model for machine side converter control system [54]

The power converter is a PWM controlled voltage source converter. The three generator reference line currents (corresponding to reference torque and flux values) are computed through the vector control scheme. In turn, the vector controller generates PWM signals through a three-phase current regulator. The model of the control scheme with current controller is shown in figure 4.7.

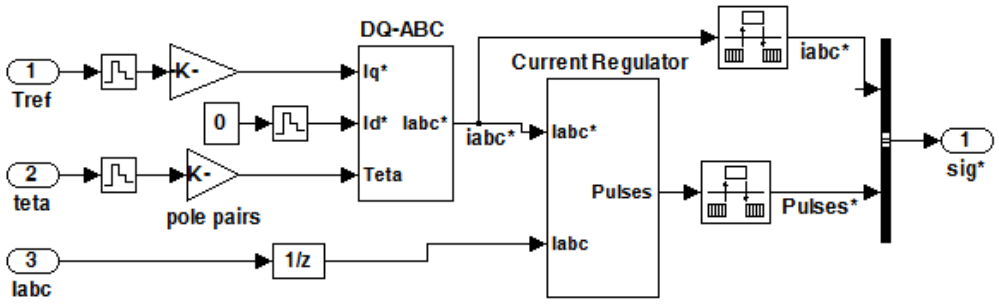

Fig.4. 7. Model of vector control scheme with current controller [54]

An optimal control is employed to regulate the line current amplitude corresponding to desired torque reference T_{ref}; consequently the nominal value of flux is maintained. The amplitude and phase of the currents are also changed in accordance with the machine torque-speed operating characteristic to achieve the desired flux weakening. A PI controller based speed control is used for obtaining torque reference. In order to achieve flux weakening control, the normalized value of flux is calculated for every change in the machine speed. The equations used to develop the control system are given below**.** Equation (34) and (35) are used in modeling simple PI-controller for speed control, equation (36) and (37) are used for modeling the inputs for the current regulator, which is a simple hysteresis controller [54].

$$\omega_{error} = \omega_{ref} - \omega_r \tag{34}$$

$$T_{ref} = K_{p\_torque}(\omega_{error}) + K_{i\_torque}\int(\omega_{error}(t))dt \tag{35}$$

$$i_q^* = \frac{2T_{ref}}{3p\phi} \tag{36}$$

$$i_d^* = 0 \tag{37}$$

The park transformation (dq to abc conversion) for I_d^* and I_q^* and electrical angle is used for calculating the stator reference current I_{abc}^*. By using I_{abc}^* and three phase stator current I_{abc}, the current regulator produces control signals for power converter. Thus the machine is controlled through power converter by using a vector control scheme.

B) Load Side Converter Control System

The load side converter control system is developed to regulate the load voltage by regulating the DC-link voltage V_{dc}. The developed control system model for load side converter is shown in figure 4.8.

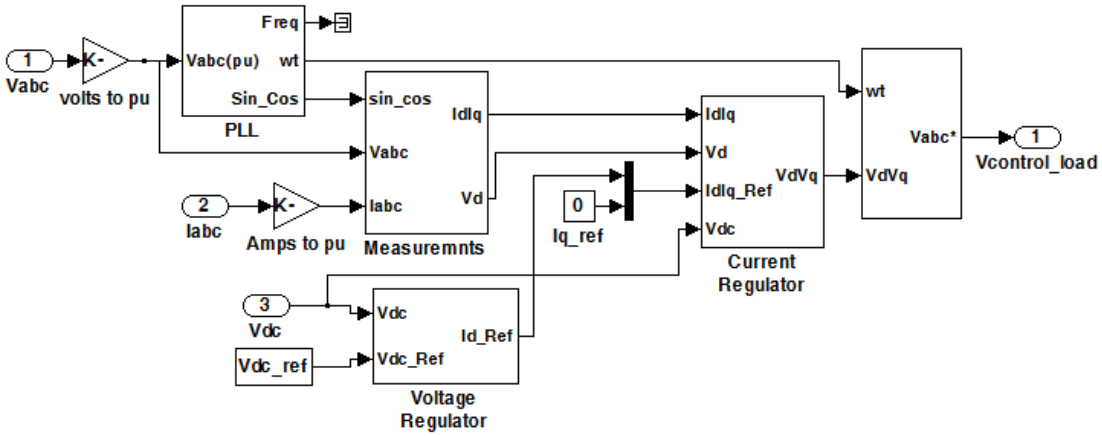

Fig.4. 8. Simulation model for load voltage converter control system [54]

The vector control scheme is employed for the load side converter. The complete control system is divided into two parts: a) voltage regulator and b) current regulator. Equations (38) to (40) are used in modeling a PI-controller for voltage regulation and equations (41) to (44) are used in developing the current regulator shown in figure 4.9 [54].

$$V_{dc\_error} = V_{dc\_ref} - V_{dc} \tag{38}$$

$$I_{d\_ref} = K_{p\_Vdc}(V_{dc\_error}) + K_{i\_Vdc}\int (V_{dc\_error})dt \tag{39}$$

$$I_{q\_ref} = 0 \tag{40}$$

Where V_{dc}, V_{dc_ref} , V_{dc_error} are dc-link voltage, reference dc-link voltage and dc-link voltage error respectively. I_{d_ref}, I_{q_ref} are reference d and q current components respectively. K_{p_Vdc}, K_{i_Vdc} are proportional and integral gains of PI controller respectively.

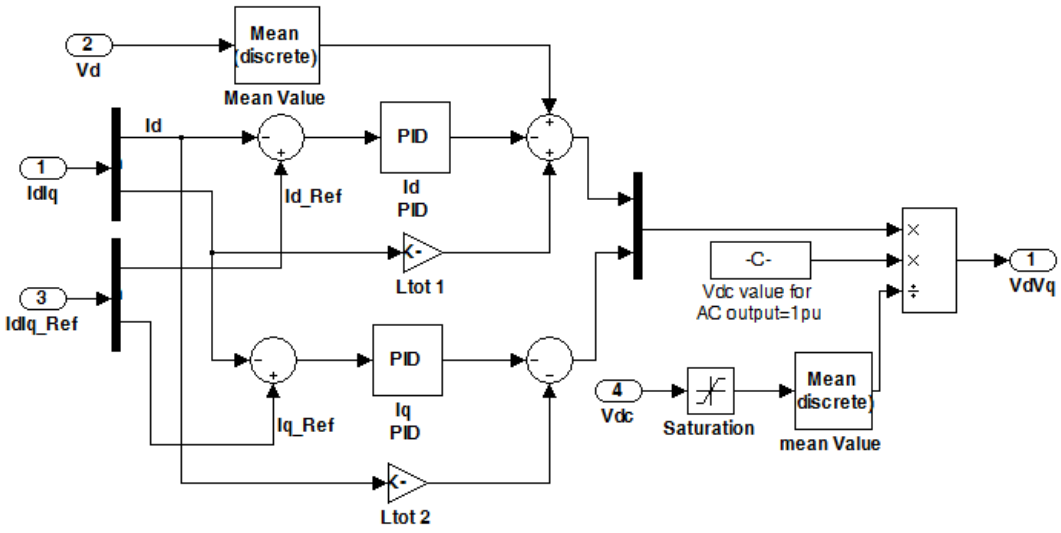

Fig.4. 9. Model of current regulator [54]

$$I_{d\_error} = I_{d\_ref} - I_d \tag{41}$$

$$V_d^{'} = V_d - \left[K_{p\_CR}(I_{d\_error}) + K_{i\_CR}\int (I_{d\_error})dt\right] + LI_q \tag{42}$$

$$I_{q\_error} = I_{q\_ref} - I_q \tag{43}$$

$$V_q^{'} = -\left[K_{p\_CR}(I_{q\_error}) + K_{i\_CR}\int (I_{q\_error})dt\right] - LI_d \tag{44}$$

Where K_{p_CR}, K_{i_CR} are the proportional and integral gains of the PI controller used for providing values of $V_d^{'}$ and $V_q^{'}$. I_d and I_q are the d and q current components respectively, obtained using park transformation (abc to dq0) for the three phase load current I_{abc_load}. The control voltage $V_{control\_load}$ used for PWM generation is obtained by applying transformation to $V_d^{'}$ and $V_q^{'}$.

4.3.2. Squirrel-Cage Induction Generator Based Stand-Alone WECS

The modelling of the squirrel-cage induction generator (SCIG) is discussed in section 3.2.1.2 of Chapter 3. In this section, the control system is developed to control the power converters at generator end and the load end. The complete simulation model of the system is shown in figure 4.10.

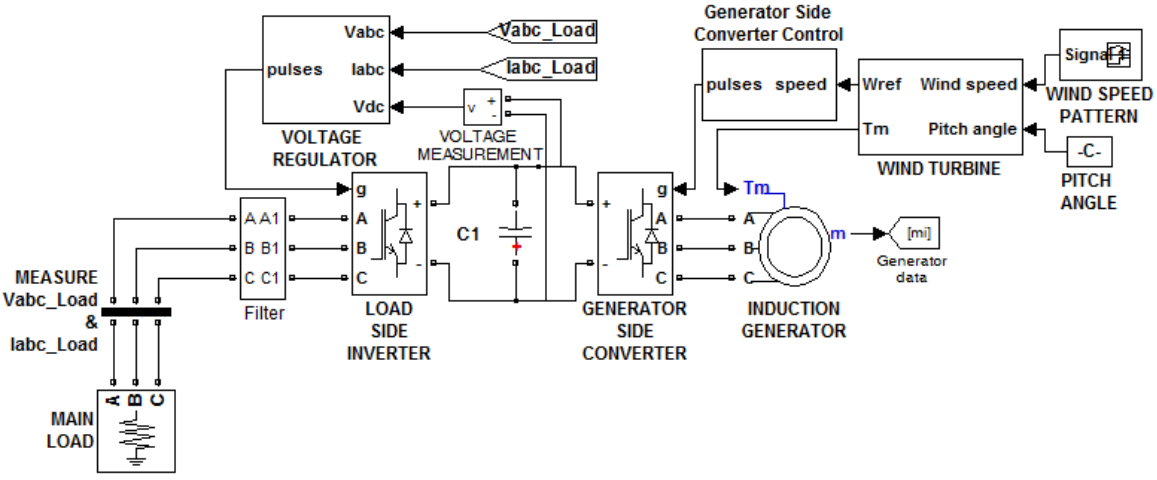

Fig.4. 10. Simulation model for SCIG based wind energy conversion system

A) Generator Side Converter Control

A vector control scheme is employed to control the generator-side power converter and minimize the difference between the rotor speed ω_r and reference speed ω_{ref}. To achieve output power control, the rotor currents are controlled in order to control the speed and torque of the induction machine. The complete model of the developed control system is shown in figure 4.11 [54].

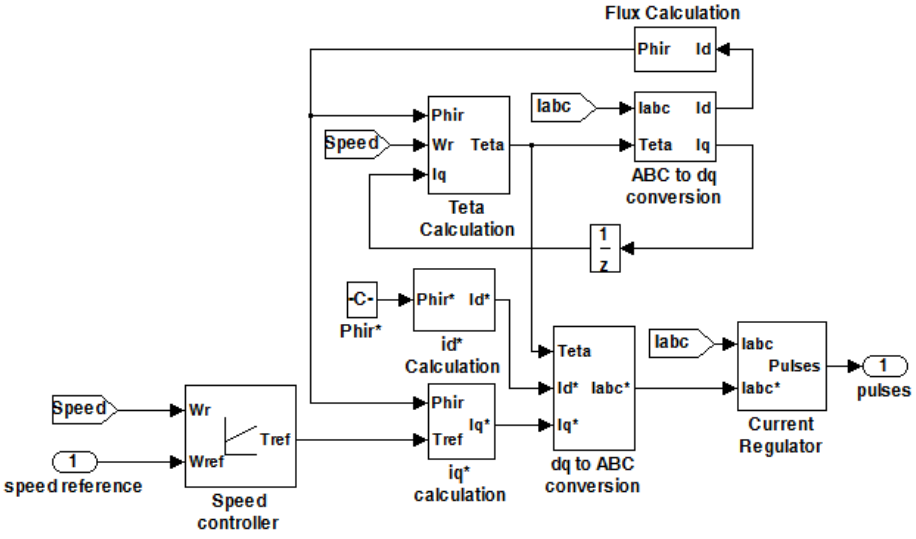

Fig.4. 11. Model of generator side converter control system [54]

By using the rotor as the reference frame, the speed control of the induction machine is achieved by a PI controller with rotational speed error as input is used to produce reference electromagnetic torque T_{ref}.

$$\omega_{error} = \omega_{ref} - \omega_r \tag{45}$$

$$T_{ref} = K_{p\_speed}(\omega_{error}) + K_{i\_speed}\int(\omega_{error}(t))dt \tag{46}$$

Using the three phase stator current I_{abc}, the value of I_q and I_d are calculated with Park transformation (abc to dq transformation). Equation (47) and (48) are used in calculation of flux ϕ_r , equations (49) and (50) are used for calculation of electrical angle θ [54].

$$\phi_r(s) = \frac{L_m I_d}{(1+\tau.s)} \tag{47}$$

$$\tau = \frac{L_r}{R_r} \tag{48}$$

Where τ the time constant, L_r is the rotor inductance, R_r is the rotor resistance and s is the Laplace variable.

$$\theta = \int(w_r + \omega_r)dt \tag{49}$$

$$w_r = \frac{L_m I_q}{\tau\phi_r} \tag{50}$$

Where w_r is the rotor frequency in (rad/s). The reference dq-axis currents are calculated using the below equations [54].

$$I_q^* = \frac{4p}{3}\frac{L_r T_e}{L_m \phi_r} \tag{51}$$

$$I_d^* = \frac{\phi_r^*}{L_m} \tag{52}$$

The Park transformation (dq to abc conversion) for I_d^* and I_q^* and θ is used for calculating the stator reference current I_{abc}^*. By using I_{abc}^* and I_{abc}, the current regulator (a simple hysteresis controller) produces control signals for power converter. Thus the rotational speed of the machine is controlled through power converter by using vector control scheme.

B) Load Side Converter Control

A vector control scheme is employed to regulate the load voltage by regulating the DC-link voltage V_{dc}. Figure 4.12 shows the control system schematic used for load voltage regulation. The input variables to the control system are V_{dc} , load voltage V_{abc}, load current I_{abc} and reference dc-link voltage V_{dc_ref} . The output of the control system provides the reference signal, used as the input for the PWM signal generator. Generated PWM signal is used as the firing pulse for the load side converter. For each sample time the V_{dc} is measured and compared with V_{dc_ref}, and the voltage regulator reduces the difference between V_{dc} and V_{dc_ref} until the voltage across the load is regulated to the desired voltage. Since the control scheme is similar to the one used for PMSG based WECS in section 4.3.1, the equations (38) to (44) are applicable for this control scheme also. The Simulink model of the load side converter control system is shown in figure 4.13.

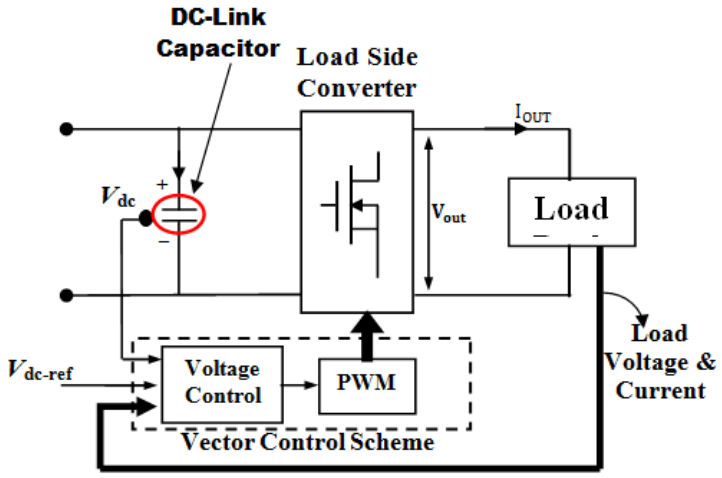

Fig.4. 12. Schematic for load voltage regulation system

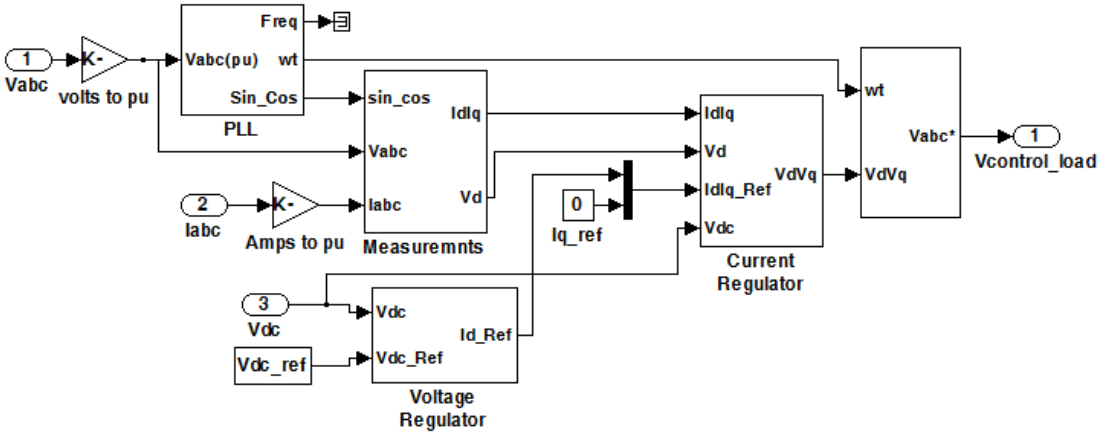

Fig.4. 13. Simulation model for load side converter control system [54]

4.3.3. Grid Connected DFIG based WECS

The modelling of the generator is discussed in section 3.2.1.2 of Chapter 3. The complete simulation model developed for the DFIG based wind energy conversion system is shown in figure 4.14 [54].

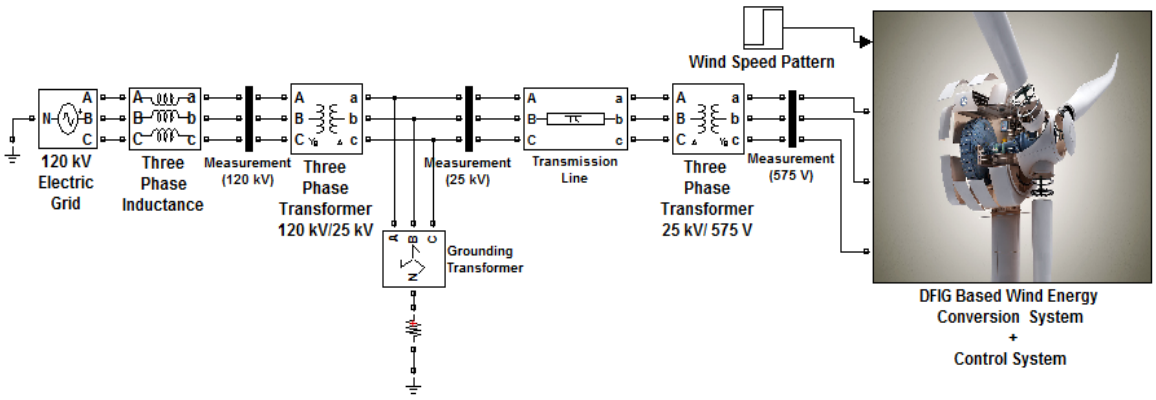

Fig.4. 14. Simulation model of grid connected DFIG based WECS

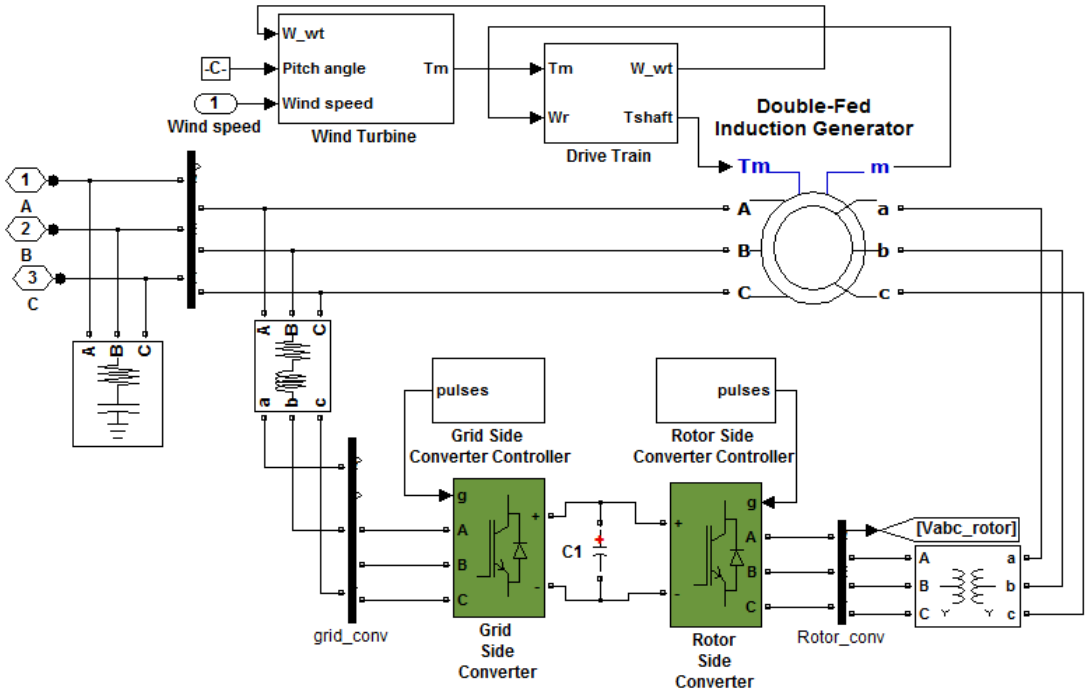

Fig.4. 15. Model of DFIG based WECS with control system

The power converters play a major role in providing dynamic control access to the DFIG. By decoupling the electrical power system frequency and mechanical rotor speed, the power converters allow variable-speed operation of WECS [63]**.** A rotor reference

frame is chosen for using Park transformation in the modeling. Control system for the rotor side and grid side converter is shown in figure 4.15 [54] and discussed in following subsections.

The electrical grid system is modeled using the following components: a) 120 KV three phase voltage source, b) three phase inductance, c) two three phase transformer, d) grounding transformer and e) three phase transmission line with pi-section model. The model of the grid is shown in figure 4.14. Detailed specification of the components is provided in the appendix.

A) Rotor Side converter Control

Rotor side converter control scheme mainly provides torque control for DFIG. The torque controller modifies the electromagnetic torque T_{em} of DFIG in correspondence to change in wind speeds, in turn controls the rotor speed to operate at desired value. From a reference rotor speed ω_{ref} value, a reference torque T_{ref} is obtained. Then a current regulator is developed for producing control signals for the rotor side converter. The developed control system model for rotor side converter is shown in figure 4.16 [54].

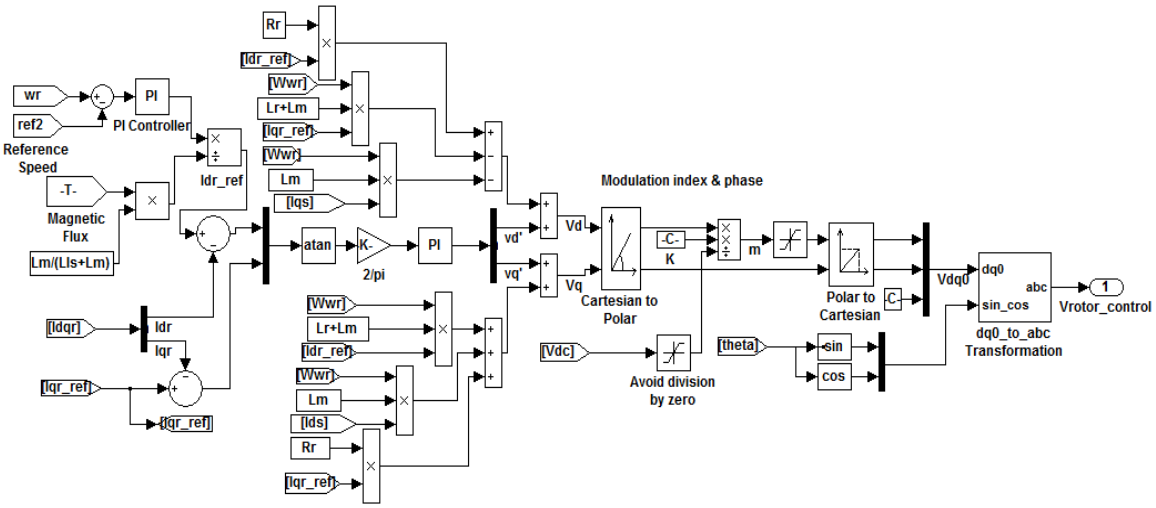

Fig.4. 16. Model of rotor side converter control system [54]

Equation (53) & (54) are used in developing an electromagnetic torque controller and equation (55) to (63) is used in developing current regulator [54].

$$\omega_{error} = \omega_{ref} - \omega_r \tag{53}$$

$$T_{ref} = K_{p\_torque}(\omega_{error}) + K_{i\_torque}\int(\omega_{error}(t))dt \tag{54}$$

$$I_{dr\_ref} = \frac{T_{ref}(L_s + L_m)}{\phi_S L_m} \tag{55}$$

$$I_{dr\_error} = I_{dr\_ref} - I_{dr} \tag{56}$$

$$I^*_{dr\_error} = \frac{2}{\pi}\arctan(I_{dr\_error}) \tag{57}$$

$$V_d^{'} = K_{p\_CR}(I^*_{dr\_error}) + K_{i\_CR}\int(I^*_{dr\_error})dt \tag{58}$$

$$I_{qr\_error} = I_{qr\_ref} - I_{qr} \tag{59}$$

$$I^{*}_{qr\_error} = \frac{2}{\pi}\arctan(I_{qr\_error}) \tag{60}$$

$$V_q^{'} = K_{p\_CR}(I^{*}_{qr\_error}) + K_{i\_CR}\int (I^{*}_{qr\_error})dt \tag{61}$$

$$V_d^{*} = V_d^{'} + \left[I_{dr\_ref}.R_r - I_{qr\_ref}.\omega_{\omega r}.(L_r + L_m) - \omega_{\omega r}.L_m.I_{qs}\right] \tag{62}$$

$$V_q^{*} = V_q^{'} + \left[I_{qr\_ref}.R_r + I_{dr\_ref}.\omega_{\omega r}.(L_r + L_m) + \omega_{\omega r}.L_m.I_{ds}\right] \tag{63}$$

Where I_{qs} and I_{ds} are estimated values, $\omega_{\omega r}$ is the difference between per unit values of system frequency and rotor speed respectively. By applying modulation index and phase conversion to V_d^{*} and Vq^{*}, the values of V_d and V_q are obtained. Then by using Park transformation (dq to abc conversion), the control voltage $V_{rotor\_control}$ is calculated and used for generating PWM signals for rotor side converter.

B) Grid Side converter Control

The grid side converter (GSC) control system regulates the DC-link voltage and in turn regulates the load voltage. The complete schematic of the grid side converter control system is shown in figure 4.17.

Vector control scheme is employed for the GSC converter. The complete GSC control system is divided into two parts: a) dc-link voltage regulator and b) current regulator. The equations used for developing the control system are provided below. Equations (64) to (66) are used in developing voltage regulator and equations (67) to (70) are used in developing current regulator [54].

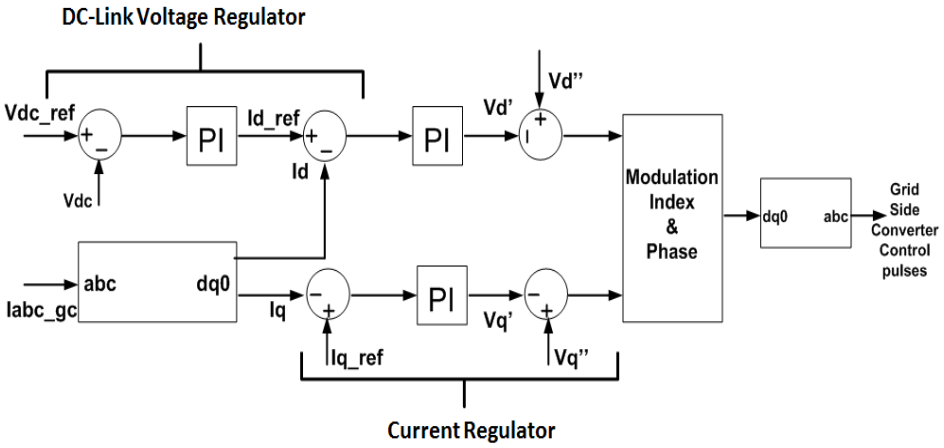

Fig.4. 17. Grid side converter control system

$$V_{dc\_error} = V_{dc\_ref} - V_{dc} \tag{64}$$

$$I_{d\_ref} = K_{p\_Vdc}(V_{dc\_error}) + K_{i\_Vdc}\int (V_{dc\_error})dt \tag{65}$$

$$I_{q\_ref} = 0 \tag{66}$$

Where V_{dc}, V_{dc_ref} , V_{dc_error} are dc-link voltage, reference dc-link voltage and dc-link voltage error respectively. I_{d_ref}, I_{q_ref} are reference d and q components of the grid current respectively. K_{p_Vdc}, K_{i_Vdc} are proportional and integral gains of PI controller respectively, used for providing I_{d_ref}.

$$V_d^{'} = K_{p\_gc\_CR}(I_{d\_ref} - I_d) + K_{i\_gc\_CR}\int (I_{d\_ref} - I_d)dt \tag{67}$$

$$V_q^{'} = K_{p\_gc\_CR}(I_{q\_ref} - I_q) + K_{i\_gc\_CR}\int (I_{q\_ref} - I_q)dt \tag{68}$$

$$V_d^{'''} = V_d + (L_{Grid})(\omega)(I_{q\_ref}) - (R_{Grid}.I_{d\_ref}) \tag{69}$$

$$V_q^{'''} = V_q - (L_{Grid})(\omega)(I_{d\_ref}) - (R_{Grid}.I_{q\_ref}) \tag{70}$$

Where $K_{p\_gc\_CR}$ *and* $K_{i\_gc\_CR}$ are the proportional and integral gains of the PI controller used for providing $V_d^{'}$ and $V_q^{'}$. I_d and I_q are the d and q components of grid current respectively, obtained using park transformation (abc to dq0) for the three phase grid current I_{abc_gc} . L_{Grid} and R_{Grid} are the grid side coupling inductance and resistance respectively.

By applying modulation index and phase conversion to $V_d^{''}$ and $Vq^{''}$, the values of V_d and V_q are obtained. Then by using Park transformation (dq to abc conversion), the control voltage $V_{grid\_control}$ is calculated and used for generating PWM signals for grid side converter.

Chapter 5

Hybrid Wind Diesel Control System

5.1. Introduction

A hybrid wind diesel system (HWDS) is a power generation system using a combination of a wind turbine generation (WTG) system and diesel generation (DG) unit as its power source. The idea is to supply the maximum portion of the load requirements from the intermittent source of wind, while supplying quality electrical power [8].

5.1.1. Types of Penetration Levels in HWDS

A) Low Penetration

In this type of HWDS, the wind power generation is just an additional source that does not require any special arrangements. With a given control flexibility of WTG system and speed of modern DG unit, the control system technology requirements are trivial for this generation level. Major operating characteristics are: a) diesel generation unit operates full-time, b) net load on diesel system is reduced by wind power generation system, c) does not requires any supervisory control system and d) peak instantaneous penetration is less than 50 percent. Figure 5.1 shows a typical low penetration HWDS [64].

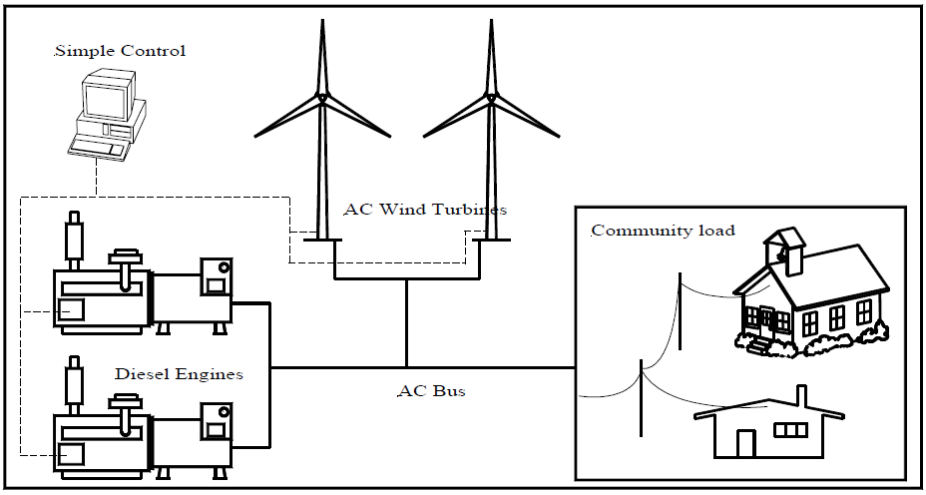

Fig.5. 1. Low penetration hybrid wind diesel system [64]

B) Medium Penetration

HWDS with large amount of contribution from wind belongs to this classification. A typical medium penetration HWDS is shown in figure 5.2 [64]. With the power penetration up to 50%, the diesel generators are loaded less than the actual capacity and sometimes it is shut off or switched to a smaller unit for production. Maintaining sufficient power balance between wind energy penetration and diesel generation becomes challenging, as operating diesel generation units to tightly regulate system voltage is difficult. However, the power quality can be improved by: a) exercising reduction of power with wind turbine control system, b) using additional loads to avoid excessive amount of energy generated by wind turbine system and c) implementing power factor correction scheme using capacitor banks or using power electronic based reactive power compensators such as STATCOM, STATIC VAR etc.

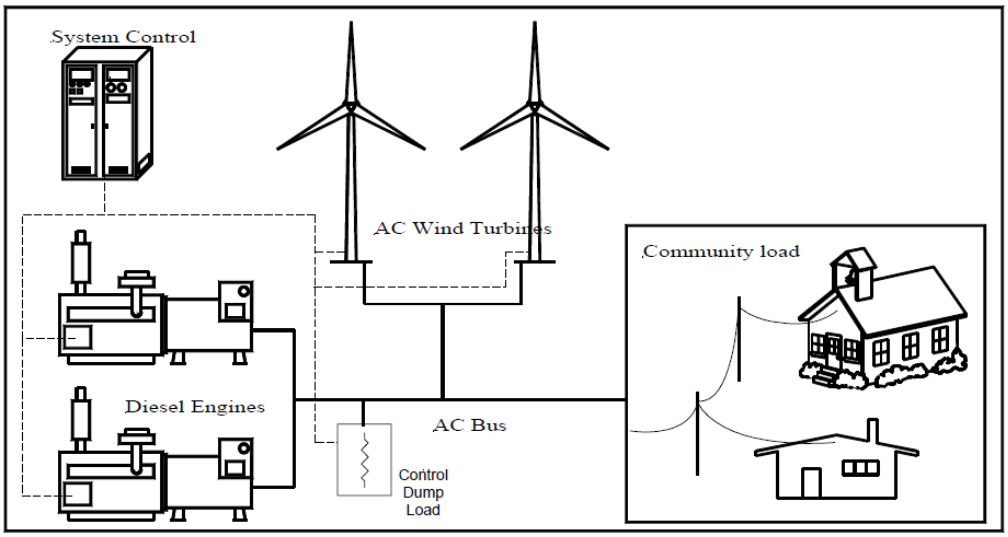

Fig.5. 2. Medium penetration hybrid wind diesel system [64]

C) High Penetration

In this type of HWDS, much auxiliary equipment are installed in addition to wind turbine to completely shut off the diesel generation unit in case of excessive power production from wind. Controllable secondary loads are used when extra instantaneous power exceeding the electrical load requirement is generated, were the instantaneous penetration is over 100%.

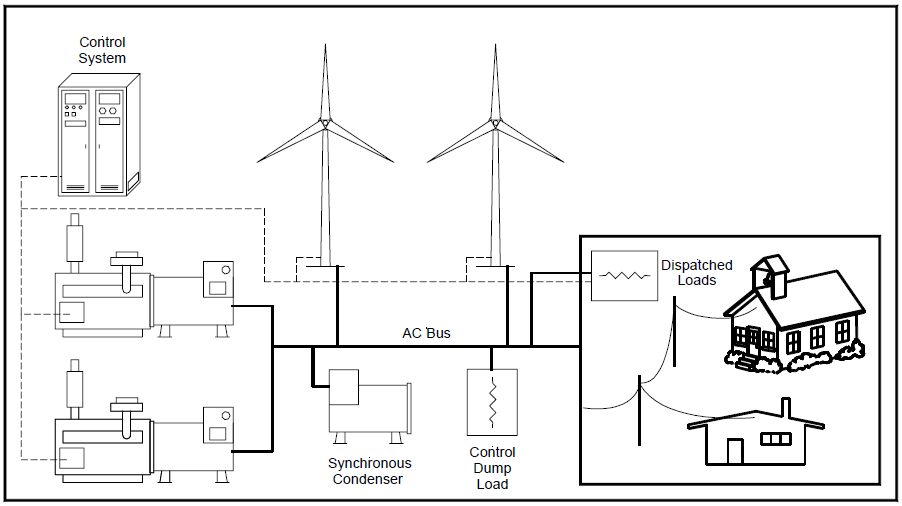

Fig.5. 3. High penetration hybrid wind diesel system [64]

The major components of the high penetration HWDS includes: power converters, synchronous condensers, load banks, dispatchable loads, battery based storage system and advanced control system to maintain system integrity and higher power quality. The high penetration systems are yet to reach the status of mature technology; this is due to the requirements like complex technology and high level system integration. But still commercially demonstrated projects are available today. Figure 5.3 shows a typical high penetration HWDS [64].

5.1.2. Modes of Operation of HWDS

A) Wind-Only Mode

In wind-only (WO) mode, the consumer load power demand is supplied by the wind turbine generation (WTG) system only. If the wind turbine is a fixed-pitch constant speed type system, no control system is employed to regulate the generated power. In order to

regulate the frequency in this mode, the variable dump load system is used. Dump load system consist of resistor/heating elements, they are connected to HWDS by power electronics switches like IGBT, GTO etc. When wind speed is high, the required dump loads are switch ON for dumping the excessive generated power, and in turn the power system frequency is maintained at constant value. If the wind turbine is a variable-pitch variable speed type system, then the pitch angle control system is used to control the wind turbine from generating excessive power during higher wind speed, in turn the frequency is maintained at predefined limits. A HWDS is operated in WO mode only when the wind power generated is greater than that of the consumer load power demand**.**

B) Wind-Diesel Mode

In wind-diesel (WD) mode of operation, both diesel generation (DG) system and WTG system are operated simultaneously to supply the consumer load power demand. The power generated by the DG system is regulated by the governor control system to supplement the power generated by the WTG system. The terminal voltage of the HWDS is regulated by the synchronous machine in diesel generation system. In this mode the diesel generator is operated continuously, even though the wind speed is high. Intermittent wind diesel mode is used for reduction in the fuel cost and the diesel governor is engaged or disengaged with synchronous generator by a mechanical clutch. Operating cost of the HWDS in the continuous wind diesel mode is much more expensive that the intermittent wind diesel mode. In general supplying a load less than 40% of the rated capacity of the diesel generator is not considered a good financial option. For

reducing the cost of operation, control systems are designed to optimize the power generation from WTG and DG.

5.2. Diesel Generator

The diesel generator consists of a diesel engine with the governor control system and a synchronous machine driven by the diesel engine. Major components of the diesel engine model consist of a controller, actuator and a delay. The diesel engine model consists of: a) a controller for checking the steady-state error in speed and b) an actuator with gain K, time constant T_i and integrator altogether for controlling the fuel rack position [65].

The diesel engine model is developed with second order controller and actuator with two transfer function TF1 and TF2 [66] as shown in figure 5.12. With the presence of dead time and occurrence of parameter variation in real-time diesel generation system, controlling the speed of diesel engine prime movers involves technical complexity, resulting in slow plant dynamics. The controller provides quick response at the startup and fast speed recovery during load variation. The developed diesel engine model emulates the rate of fuel consumption as a function of speed, which is modeled using a simple first order equation relating the fuel rack position and the developed mechanical power of the diesel engine [67]**.**

The governor control system plays a major role in regulating the speed of the engine and in turn the power generation by controlling the diesel's flow to the engine, so that the

required power is generated to supply the load. Variation in the dead-time together with system parameter uncertainties results in significant degradation in the performance of diesel engine as a prime mover, mainly during load changes, which is a commonly occurring change in power system [68].

The existence of the non-linear, time-varying, dead time between the fuel injection and production of mechanical torque T_{mech} makes the diesel engine a non-linear system [69]. So the speed is commonly controlled by a PI controller to prevent steady-state error in speed. The production of mechanical torque T_{mech} is represented by conversion of fuel-flow to torque after a time-delay T_d [54]. The equation used for the conversion is expressed below [54].

$$T_{mech}(S) = e^{-sT_D}\phi(S) \tag{71}$$

5.2.1. Synchronous Machine Model

The electrical system of the machine is represented by state space model. Each phase consists of a voltage source in series with RL impedance, which implements the internal impedance of the machine. The electrical quantities along with rotor parameters are referred to the stator and indicated by primed variables. Dynamics of the stator, field and damper winding are taken into consideration in the model, and the equivalent circuit is represented in the d-q rotor reference frame as shown in figure 5.4 and 5.5 respectively.

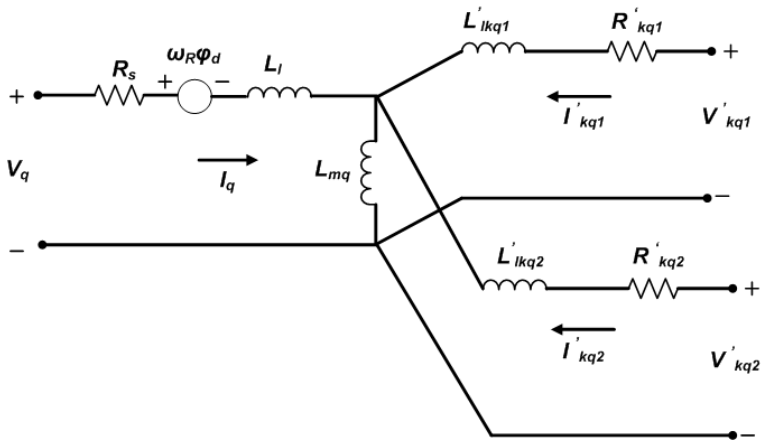

Fig.5. 4. Equivalent circuit model of electrical system of synchronous machine in q-axis frame [54]

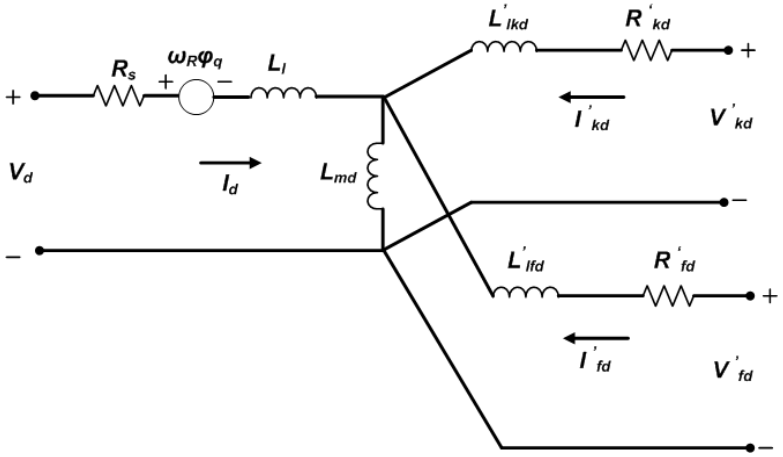

Fig.5. 5. Equivalent circuit model of electrical system of synchronous machine in d-axis frame [54]

The equations of electrical system are given below [54].

$$V_d = R_s i_d + \frac{d}{dt}(\varphi_d) - \omega_R \varphi_q \tag{72}$$

$$V_q = R_s i_q + \frac{d}{dt}(\varphi_q) + \omega_R \varphi_d \tag{73}$$

$$V_{fd}^{'} = R_{fd}^{'} i_{fd}^{'} + \frac{d(\varphi_{fd}^{'})}{dt} \tag{74}$$

$$V_{kd}^{'} = R_{kd}^{'} i_{kd}^{'} + \frac{d(\varphi_{kd}^{'})}{dt} \tag{75}$$

$$V_{kq1}^{'} = R_{kq1}^{'} i_{kq1}^{'} + \frac{d(\varphi_{kq1}^{'})}{dt} \tag{76}$$

$$V_{kq2}^{'} = R_{kq2}^{'} i_{kq2}^{'} + \frac{d(\varphi_{kq2}^{'})}{dt} \tag{77}$$

Where,

$$\varphi_d = L_d i_d + L_{md}(i_{fd}^{'} + i_{kd}^{'}) \tag{78}$$

$$\varphi_q = L_q i_q + L_{mq} i_{kq}^{'} \tag{79}$$

$$\varphi_{fd}^{'} = L_{fd}^{'} i_{fd}^{'} + L_{md}(i_d + i_{kd}^{'}) \tag{80}$$

$$\varphi_{kd}^{'} = L_{kd}^{'} i_{kd}^{'} + L_{md}(i_d + i_{fd}^{'}) \tag{81}$$

$$\varphi_{kq1}^{'} = L_{kq1}^{'} i_{kq1}^{'} + L_{mq} i_q \tag{82}$$

$$\varphi_{kq2}^{'} = L_{kq2}^{'} i_{kq2}^{'} + L_{mq} i_q \tag{83}$$

Where the subscript: a) *R* and *s* refers to rotor and stator parameters b) *l, m* refers to leakage and magnetizing inductance respectively c) *f, k refers to* field and damper winding quantity respectively.

The equations for the mechanical system are expressed below [54]:

$$\Delta\omega_R(t) = \frac{1}{2H}\int_0^t (T_m - T_e)dt - K_d\Delta\omega_R(t) \tag{84}$$

$$\omega_R(t) = \Delta\omega_R(t) + \omega_0 \tag{85}$$

Where, H is Inertia constant, T_m is mechanical torque, T_e is electromagnetic torque, K_d is damping factor representing effect of damper windings, $\omega_R(t)$ is rotor speed and ω_0 is speed of operation.

5.2.2. Excitation System

An excitation system is used for exciting the field windings of the synchronous machine and also used for regulating the terminal voltage when operated in the generator mode. The excitation system, used in this project work, is a DC exciter [70]; it is assumed that no saturation occurs in the system. The major components of the excitation system includes: a voltage regulator and an exciter circuit. The excitation system is represented by the transfer function expressed in equation (86) [54].

$$V_{fd} = \frac{E_r}{K_{ex} + sT_{ex}} \tag{86}$$

Where V_{fd} is the exciter voltage, E_r is the output of voltage regulator, K_{ex} is the exciter gain and T_{ex} is the time constant of exciter.

5.3. Control System for HWDS

The developed control system operates the HWDS in wind-only (WO) and wind-diesel (WD) mode of operation. In WO mode, the generator side converter is used for controlling the WTG to achieve maximum power point tracking (MPPT), and the frequency regulation system operates the required sink (i.e. the dump load) for the excessive generated power. In WD mode, the wind turbine is controlled using MPPT to extract maximum power from wind, and simultaneously the diesel generator (DG) unit is operated to supplement the power generation from WTG to meet the load power demand. In WD mode, the generated voltage in HWDS can also be controlled by the excitation system of the synchronous generator.

At any given time, the power generated from the wind turbine varies with the fluctuating wind speed. In a large interconnected power system, these fluctuations are absorbed by the electric grid to regulate the power system frequency. In case of low and medium penetration HWDS, which is mostly operated as an isolated power system, the power balance is maintained by controlling the power generation of the diesel generator. This also ensures that the system integrity is not disturbed.

The wind turbine is considered to be a much more complex system than the DG unit and the control system developed in this project is mostly focussed on the wind turbine. All the concepts discussed and control system developed in chapter 4 is applicable to HWDS. Two different types of power system configuration are chosen to simulate the HWDS: a stand-alone configuration and a micro-grid configuration. In the stand-alone

configuration, a PMSG based direct-driven WECS is used and a DFIG based WECS is used for the micro-grid configuration.

5.3.1. HWDS Based Stand-Alone Power System

The schematic of the control system developed for HWDS in stand-alone configuration is shown in figure 5.6. The considered hybrid power system consists of a PMSG based direct-driven wind turbine, a synchronous machine based diesel generator, power electronic converters and the dump loads. The dump loads are used as sink for excessive power generation. The control system is developed to control the power converters at the machine side and load side. A maximum power point tracking control is simulated for wind turbine with the machine side converter. In this configuration, the transition from WD to WO mode is simulated. The diesel generation system includes a governor control for controlling its power generation. The main contribution of the developed control system for this HWDS is to show: a) power sharing between the sources and the sink and b) transition between WD to WO mode of operation and c) maximum power extraction from wind that leads to reduced usage of diesel generation system.

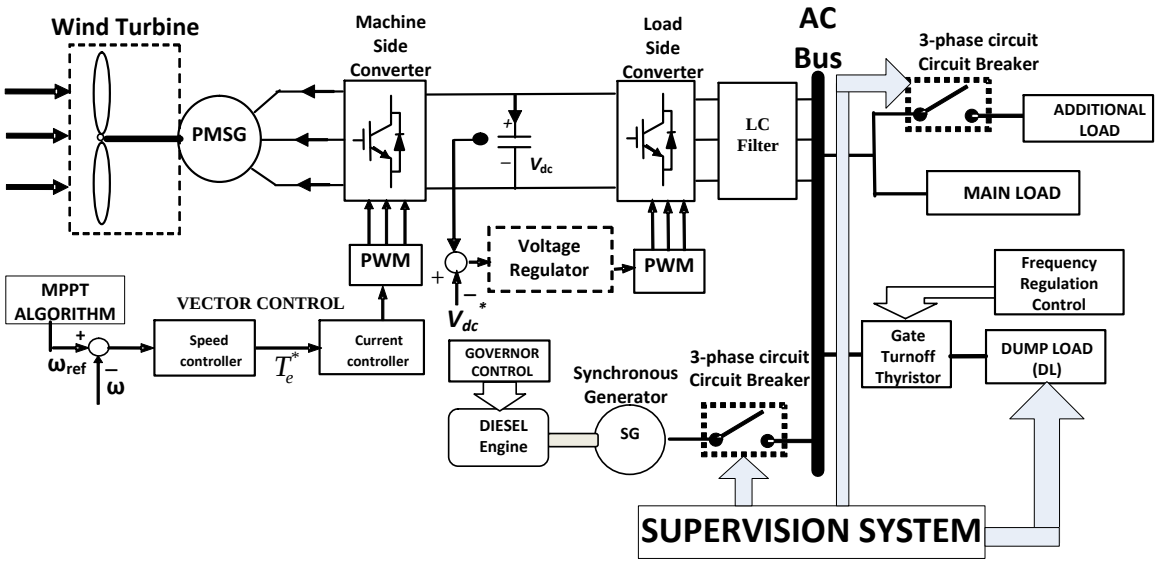

Fig.5. 6. Schematic of hybrid wind diesel system with PMSG based direct-driven WECS

The values of the parameters used for modeling the WECS and DG unit are referred from the machine specifications provided by *TechnoCentre* [4] to closely resemble its wind-diesel generation capacity used in their micro-grid project. The simulation model developed for HWDS based stand-alone power system is shown in figure 5.7.

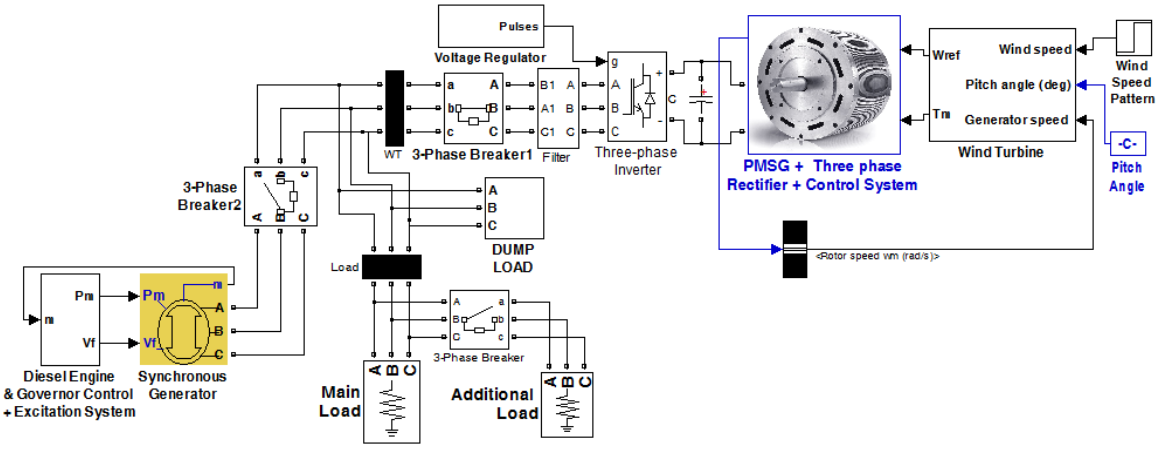

Fig.5. 7. Simulation model of HWDS based stand-alone power system

5.3.2. HWDS Based Micro-Grid Power System

The schematic of the HWDS in micro-grid configuration is shown in figure 5.8 and the simulation model is shown in figure 5.9 [54]. In this configuration, the control system is developed for operating the hybrid wind diesel based micro-grid in a) grid connected mode and b) the islanded/isolated mode. The micro-grid consist of DFIG based wind farm, synchronous machine based diesel generator and regular electric grid supply. Were it is assumed that all the wind turbines are exposed to same wind speed.

The control system is developed to control the power converters at the generator side and grid side. A maximum power point tracking control is simulated for wind turbines with the generator side converter. The developed grid side converter control system regulates the DC-link voltage. The diesel generation system includes a governor control for controlling its power generation. A supervisory control is simulated to disconnect the grid supply through a circuit breaker during isolated mode of operation. The main contribution of the developed control system for this HWDS is to show: a) power sharing between the sources and the sink and b) transition between WO to WD mode and WD to WO mode of operation, c) maximum power extraction from wind that leads to reduced usage of diesel generation system and d) regulation of DC-link voltage leading to regulated load voltage.

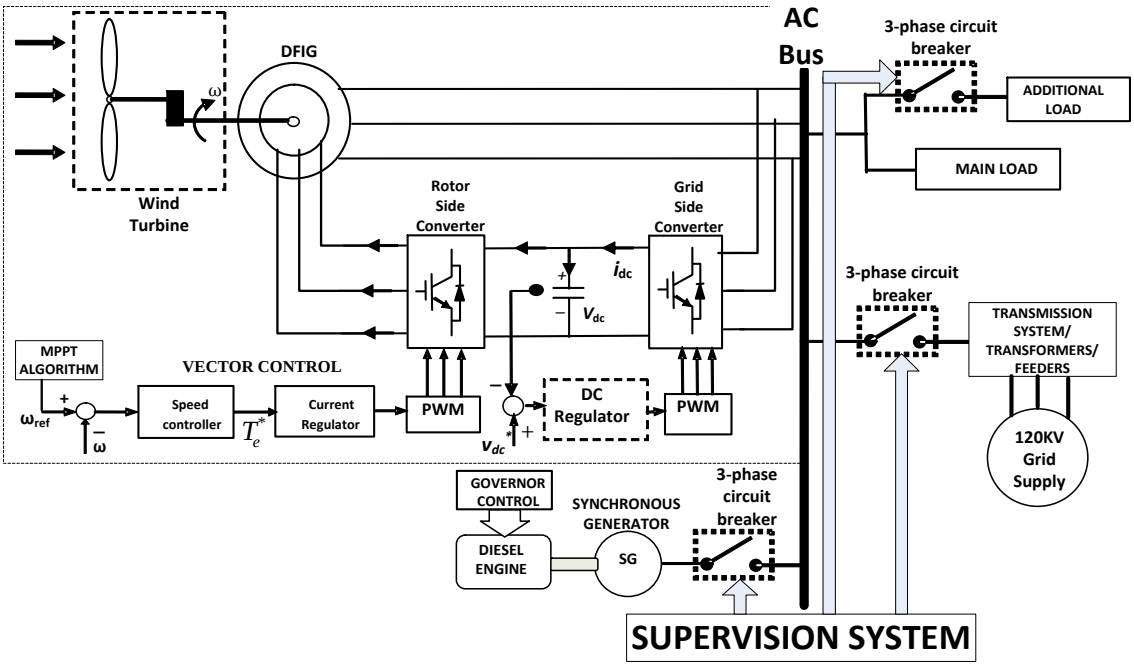

Fig.5. 8. Schematic of hybrid wind diesel system based micro-grid

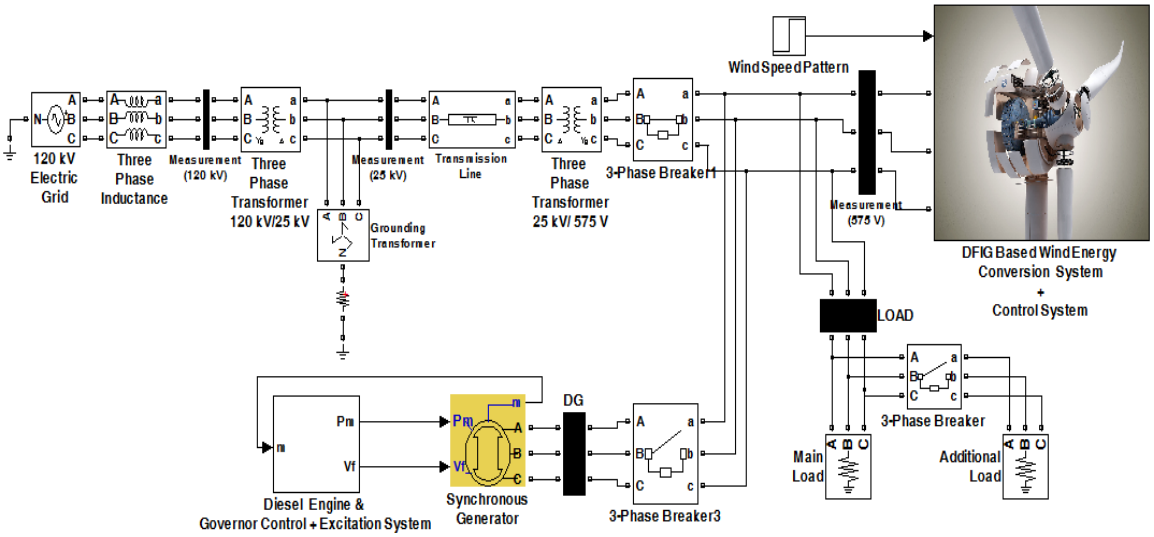

Fig.5. 9. Simulation model of HWDS based micro-grid system

5.3.3. Frequency Regulation System

Power system frequency represents the stability and balance maintained between the load power demand and the generated power. Small or large fluctuation in load power demand occurs commonly in any power system operation. Generator tripping or outage of power plants can lead to a critical stability problem and large frequency fluctuation in power system. In order to avoid these common problems and safeguard the stability of power system, a frequency regulator control system should be implemented.

The power supply frequency of the HWDS supplying the isolated load can be regulated using controlled dump loads [71]. Dump loads are variable loads that can be controlled by power electronic switches with high frequency switching action. The dump loads are modeled using eight sets of three-phase resistors connected in series with gate turn-off (GTO) thyristor switches as shown in figure 5.10, where A,B and C are the phase terminals connecting the main loads. The nominal power of each set of dump load follows a binary progression so that the dump load can be varied in ranges of values. In this simulation, frequency regulation controller is implemented only for the stand-alone HWDS configuration. In a grid connected system, various generating sources are interconnected to common bus and operated in synchronism, where the control system at each generation station regulates the system frequency to match the grid operating frequency. So in general, the wind turbine system connected to the grid is considered to be operating at constant grid frequency.

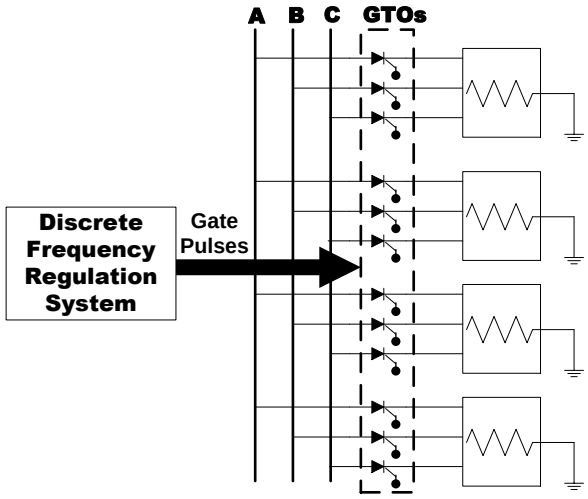

Fig.5. 10. Dump load system with four-sets of loads

The frequency is regulated by the discrete frequency regulator control system. The simulation model of the frequency regulation system is shown in figure 5.11. A standard discrete three-phase phase locked loop (PLL) system is employed to measure the frequency of power system. The measured frequency is compared to the reference frequency (60 Hz for North American standards) to obtain the frequency error. A phase error is obtained by discrete-time mathematical integration of frequency error. This phase error is then used as an input to proportional-derivative (PD) controller to produce an output signal representing the required dump load power. This signal is converted to an 8-bit digital signal using a sampling system, with each bit providing switching pulse to the GTOs connected to the eight sets of three-phase dump loads. Switching action of these dump loads are performed at zero crossing of voltage to reduce fluctuations in the voltage.

The reference frequency input for the control system has been considered as 60Hz. For each sample time, frequency of the system is measured and compared with reference frequency. Any difference in the frequency will actuate the required dump loads to minimize the error between the reference frequency and system frequency. The process continuous throughout the simulation to ensure the system frequency is maintained at 60 Hz [72].

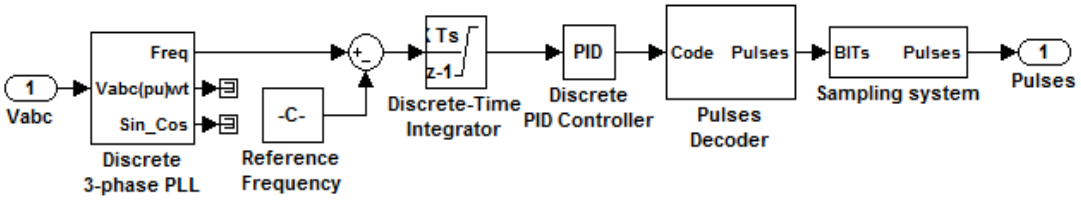

Fig.5. 11. Model of frequency regulation system [54]

5.3.4. Governor Control system for Diesel Generator

In a diesel engine, the speed of the engine is regulated by controlling the flow of diesel into the cylinders with the help of injectors, the device which performs this task of regulation is known as the governor. This is mainly responsible for regulating the speed. Regardless of any change occurring in the load, the governor has a main role in maintaining speed of engine at constant value.

For the diesel generation application, the diesel engine acts as the prime mover of a generator shaft to produce electrical power. Governor that controls the engine at constant speed regardless of the variations in the load is known as the constant speed governor. Governor that maintains the speed within a range of maximum and minimum value is known as the speed limiting governor. In this project, a constant speed governor model

[65] [66] is chosen and simulated into HWDS model, where the power applied to the generator shaft is controlled by the governor control system, which majorly involves the controlling the fuel rack position. The simulation model of the diesel engine with the governor control system is shown in figure 5.12.

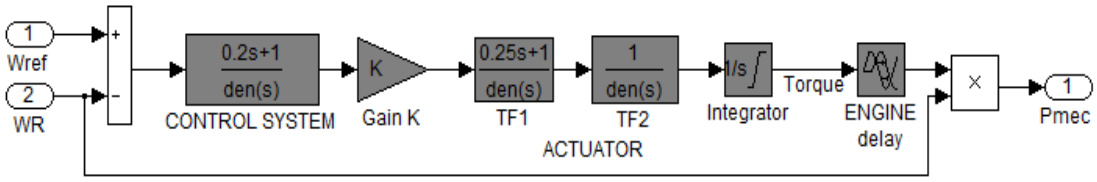

Fig.5. 12. Model of diesel engine with governor control system [54]

The main objective of the power control on the generator shaft is to regulate the speed, which is controlled for operating the diesel generator in parallel to the electric grid. When the diesel generator is operating in parallel with grid, the governor controls the power generation only and not the speed (but the behaviour of the governor varies in an isolated power system). The operating speed of diesel generator is related to the frequency of the generated voltage as given by the below expression:

$$Generator\ frequency = \frac{Speed\ of\ the\ engine\ (in\ RPM) * Number\ of\ magnetic\ poles\ in\ generator}{120}$$

Both frequency and speed can be used for controlling the governor. But control using frequency signal has a drawback, as the generator frequency signal depends upon the excitation of the generator. In case of failure in excitation system, the insufficient residual magnetism fails to provide the required signal, and the engine speed will continue

increasing till the prime mover shaft is damaged by over speed. This is avoided by using a mechanical governor or an additional control for prime mover as a backup for the electrical governor [73].

Chapter 6

Simulation Results and Discussion

6.1. Organization of Results

Validating the performance of the developed control system for the HWDS is shown by the simulation results. The results are organized as follows: the section 6.2 will discuss results obtained from the simulation models of the wind energy conversion system, the section 6.3 will discuss the results obtained from the HWDS simulation models.

In this chapter, the results obtained for the PMSG based WECS and HWDS are mainly focussed for the model validation with real-world data. The PMSG based WECS and HWDS are developed based on the real-time specifications provided by the TechnoCentre Éolien (TCE) [4]. The simulation results obtained closely conforms to the power curve of the wind turbine employed at the research unit of TCE. In order to test the control system performance, different wind speed patterns are simulated and the results obtained are presented.

6.2. Simulation Results Obtained for Wind Energy Conversion System

6.2.1. DFIG based Grid Connected Wind Energy Conversion System

Validating the performance of the developed control system (in section 4.3.4 of chapter 4) for the WECS is shown by the simulation study results. Figure 6.1 shows the speed tracking performance of the control system. A maximum power point tracking (MPPT) algorithm is simulated to track the optimum rotor speed for maximum power extraction from available wind. The first graph of figure 6.1 shows the wind speed with sharp step change occurring at 10 second simulation time. Second graph in figure 6.1 shows the speed tracking, the MPPT reference speed is calculated by an MPPT algorithm discussed in section 4.2.3 of chapter 4. It is observed that at the time zero the DFIG starts with an initial speed (150 rad/s). This initial rotor speed effect is caused by the connection of stator with electrical grid. This also has an effect during the speed transitions as seen in figure 6.1. But still the controller is able to control the rotor speed to match the reference speed; this is achieved by manual tuning of controller gains. During the simulation time from ten to thirteen seconds the power generated is close to zero, this is mainly attributed to the loss of speed tracking control. It can be observed that the actual speed fluctuates. The differences between the actual speed and the MPPT reference speed along with the influence from the grid are mainly responsible for the dip in the generated power. The control system is required to be improved.

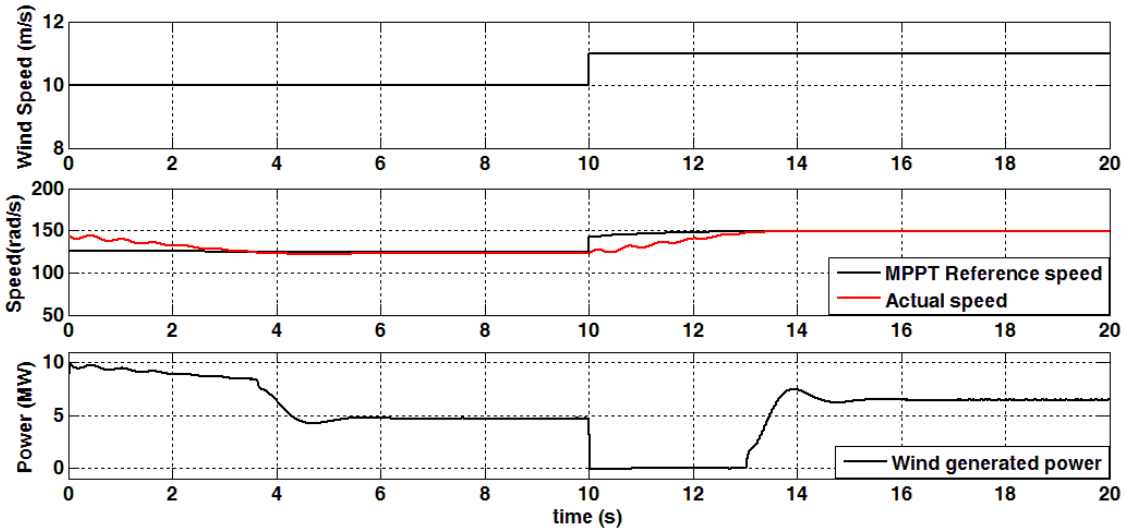

Fig.6. 1. Maximum power point tracking performance

Figure 6.2 shows the DC-link voltage regulator performance. Throughout the simulation the DC-link voltage is maintained at constant value. Hence the grid side converter control system has good performance.

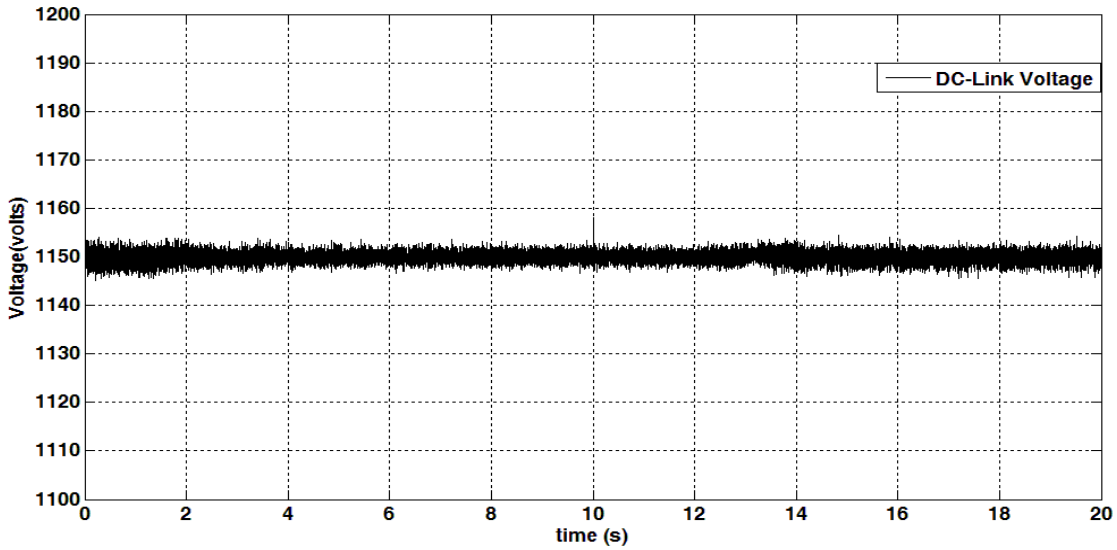

Fig.6. 2. DC-link voltage regulation

6.2.2. PMSG Based Stand-Alone Wind Energy Conversion System

Validating the performance of the developed control system (in section 4.3.2 of chapter 4) for the WECS is shown by the simulation study results. Figure 6.3 shows the speed tracking performance of the control system. A maximum power point tracking algorithm is simulated to track the optimum rotor speed for maximum power extraction from available wind. First graph of figure 6.3 shows the wind speed with sharp step change occurring at 4 second simulation time. The second graph in figure 6.3 shows the speed tracking, the MPPT reference speed is calculated by an MPPT algorithm discussed in section 4.2.3 of chapter 4. It can be observed that the performance of the speed controller is good in overcoming sharp changes in speed reference.

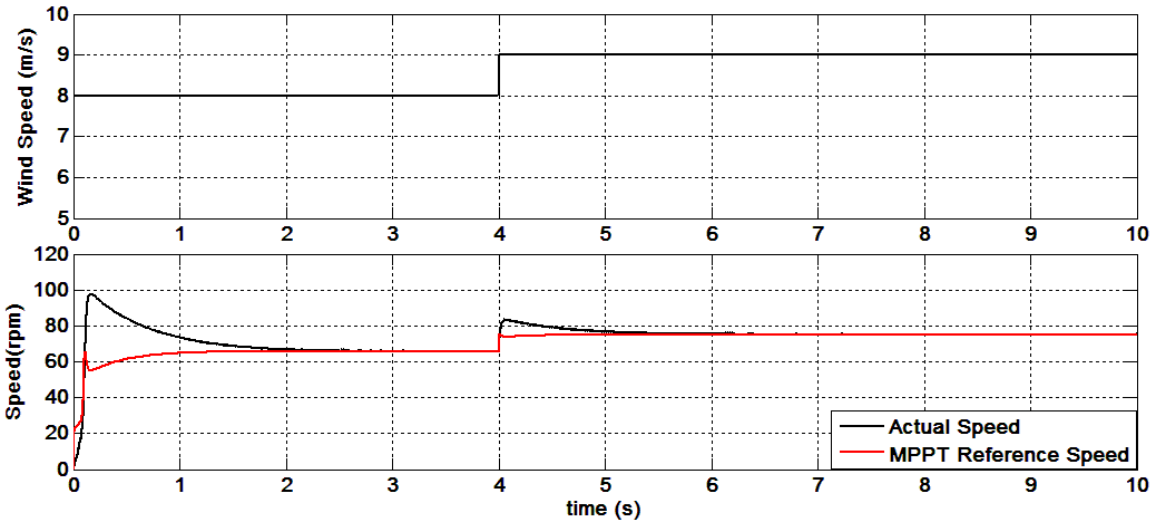

Fig.6. 3. Speed tracking performance

Figure 6.4 shows the load power consumption corresponding to wind pattern in figure 6.3. Throughout the simulation time a steady load power is supplied from WECS. An additional load is added at simulation time 7 seconds.

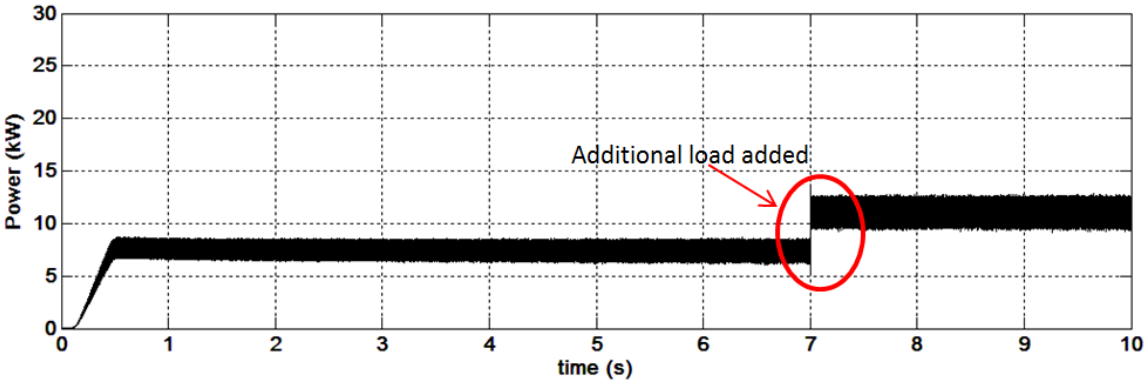

Fig.6. 4. Load power consumption

Figure 6.5 shows the regulated load voltage. A constant load voltage is maintained throughout the simulation. It can be observed that the load voltage regulator performance is good.

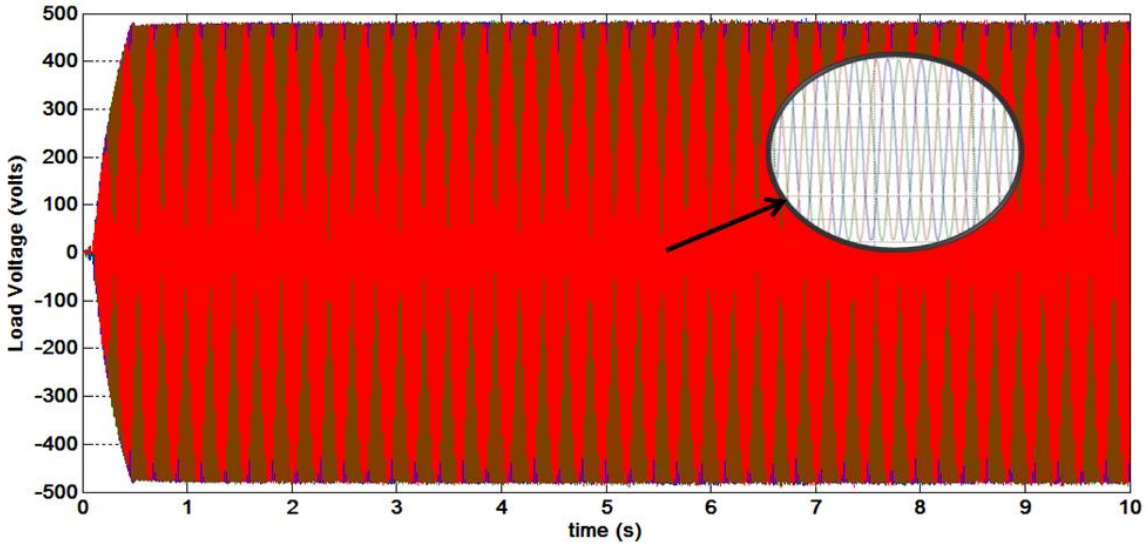

Fig.6. 5. Regulated load voltage

The wind turbine at TCE is a fixed pitch variable speed system. With a fixed pitch system, maintaining the power and speed at rated values during the above-rated wind speed regime is challenging control scenario. In order to resolve this real-world problem, the speed of the generator should be controlled to rotate at rated value through the control scheme discussed in previous chapters. The rated wind speed for the wind turbine is 11m/s. In the simulation, a step change (from 8 to 11.5m/s) in wind speed has been used to study the control system performance under the above-rated wind speed. Figure 6.6 shows the results obtained for this simulation. It can be observed that the generator speed can be controlled at closer to rated values even under above-rated wind speed regime.

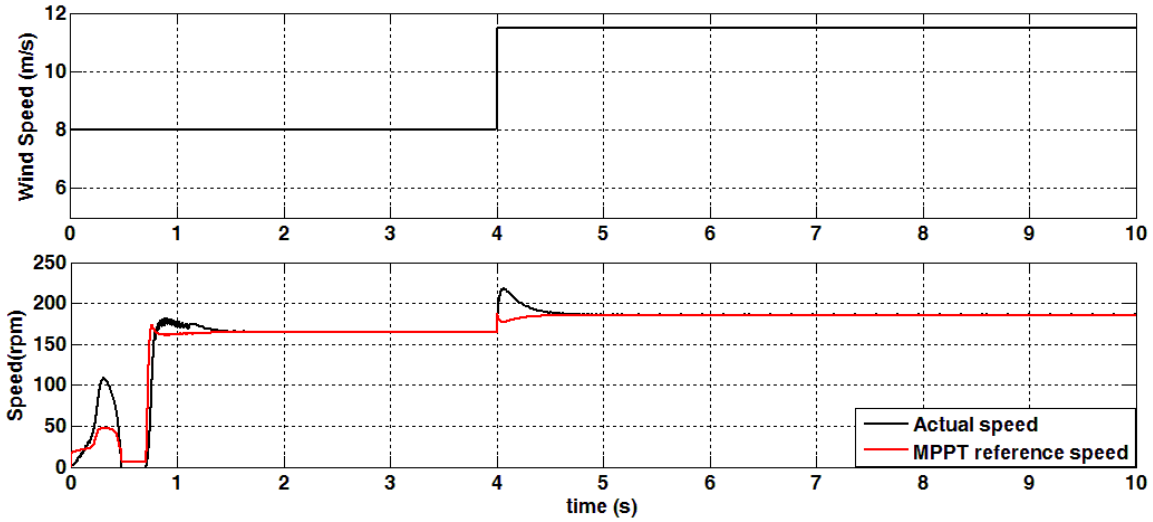

Fig.6. 6. Speed tracking performance under above-rated wind speed regime

Figure 6.7 below shows the control system performance for a sine wave shaped wind speed pattern. The first graph shows the wind speed. The second graph shows the MPPT speed tracking performance of the controller. It can be observed that the performance of

the controller requires an improvement; this can be achieved by tuning of the controller. The transient observed before one second simulation time is mainly attributed to the chosen initial values of power and speed in the MPPT algorithm discussed in section 4.2.2 of chapter 4. Still it can be observed that the generator rotor speed is controlled to track the change in the MPPT reference speed.

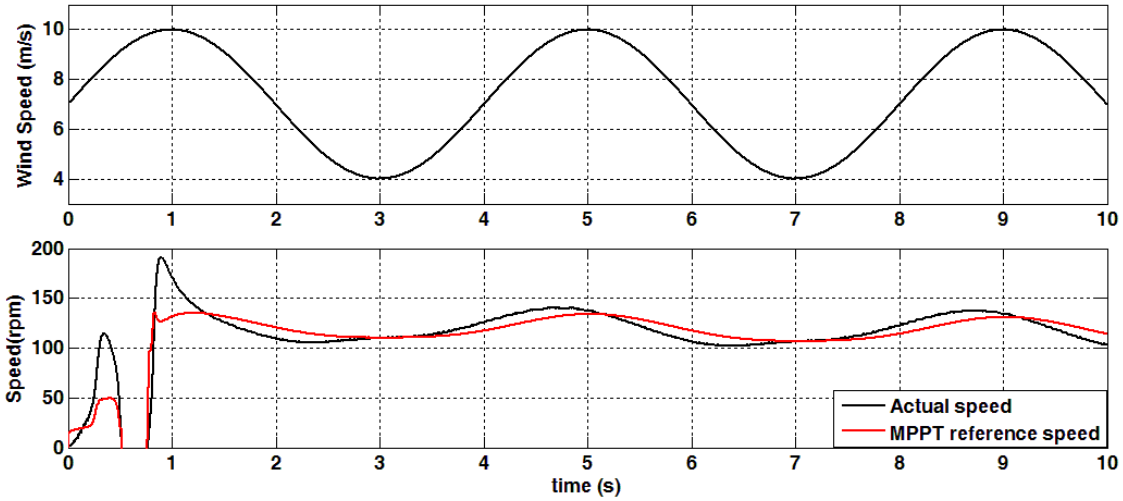

Fig.6. 7. Speed tracking performance under sine wave shaped wind speed pattern

Figure 6.8 shows the load power consumption corresponding to the wind speed pattern shown in the above graph. The initial load is 10kW and an additional load connected through a circuit breaker at 7^{th} second. It can be observed that, the load power supply is kept constant even under the fluctuating wind speed. This is mainly achieved through the usage of power converters. But the graph shows that the power supplied is slightly lesser than the load demand, this is mainly attributed to the losses incurred in the power filter and other components the system.

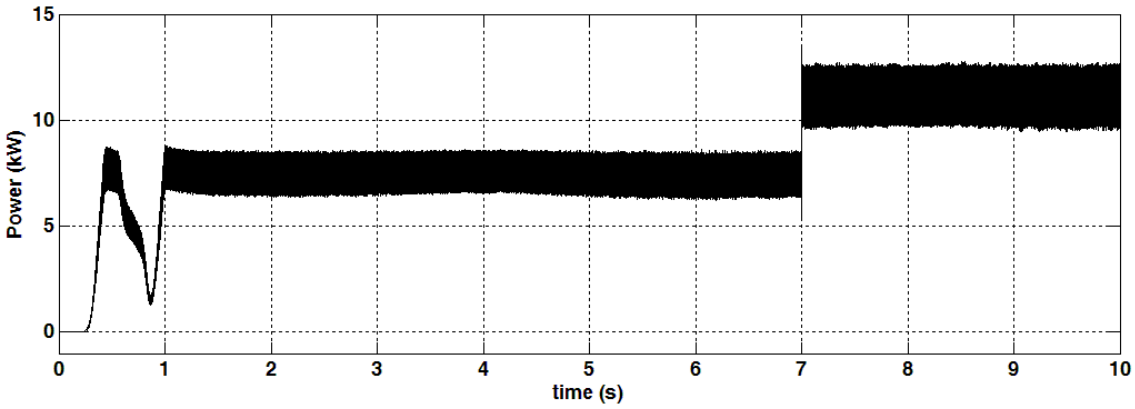

Fig.6. 8. Load power consumption

Figure 6.9 shows the graph for the load voltage regulation. The significance of the load voltage regulation is related to the power quality supplied to the load. Any load connected to a source is required to be supplied with constant voltage at rated value. The result observed in the graph corresponds to the wind speed pattern shown in figure 6.7. The rated load voltage is 480V and it can be observed that the load voltage after 1st second is kept constant at 480V throughout the simulation under changing wind speeds. The values of the load voltage observed before 1st second contains a mild fluctuation, this is attributed to the transient behaviour observed in the second graph of figure 6.7. During the transient period, the controller is yet to track the MPPT reference speed, the difference between the actual speed and the reference speed influences the generated voltage and in turn responsible for the load voltage fluctuation.

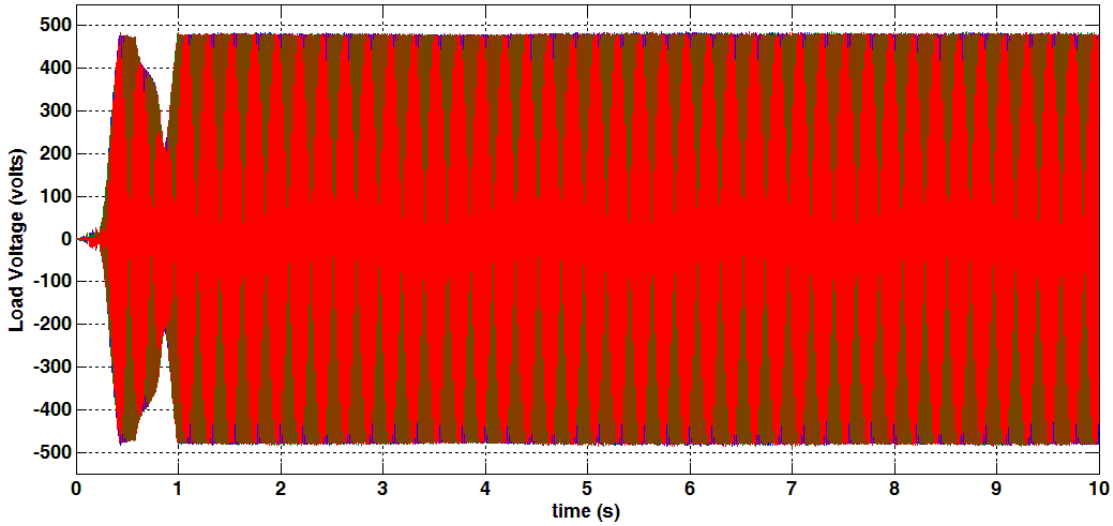

Fig.6. 9. Regulated load voltage

6.2.3. SCIG Based Stand-Alone Wind Energy Conversion System

Validating the performance of the developed control system (in section 4.3.3 of chapter 4) for the WECS is shown by the simulation study results. Figure 6.10 shows the speed tracking performance of the control system. The first graph shows the sinusoidal wind speed pattern. The second graph in the figure 6.10 shows the speed tracking performance of the controller. Where the reference speed is generated from the MPPT control scheme described in section 4.2.3 and the actual speed is the speed of the generator. It can be observed that the speed tracking performance is good. This shows the wind turbine operates at higher power coefficient in turn higher efficiency in terms of power conversion.

The third graph in the figure 6.10 shows the power generated by wind turbine system. The power fluctuation is attributed to the wind speed pattern variation and speed tracking

control action with MPPT control scheme. Since the system is operated in stand-alone mode, the load power consumption is equal to the wind turbine power output. Occurrence of power fluctuations at the load end power converter is reduced by LC filters.

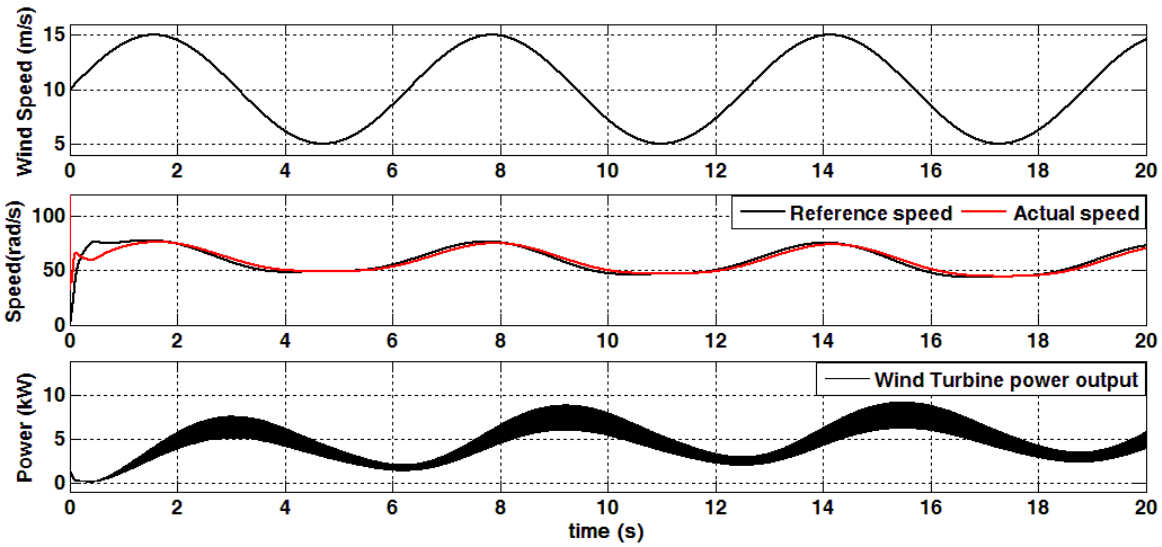

Fig.6. 10. Speed tracking performance of the control system

Figure 6.11 shows the control system performance for load voltage regulation. The load voltage is regulated at constant value. It can be observed that the performance of voltage regulator maintains the load voltage at a constant value (≈400V).

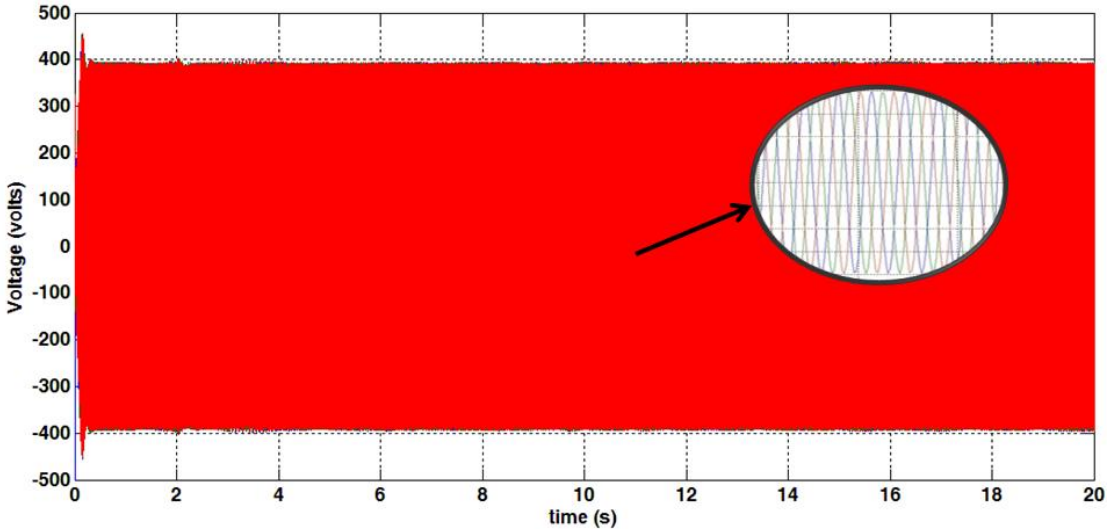

Fig.6. 11. Regulated load voltage

6.3. Simulation Results Obtained for Hybrid Wind Diesel System

6.3.1. Stand-Alone Hybrid Wind Diesel System with PMSG based WECS

Validating the performance of the control system discussed (in section 5.3.1 of chapter 5) for the HWDS is shown by the simulation study results. Figure 6.12 shows the speed tracking performance of the control system. The first graph of figure 6.12 shows the step change (occurring at simulation time 6.5 sec) in wind speed. The second graph of shows speed tracking to achieve maximum power extraction, were the reference speed is generated using the MPPT algorithm discussed in section 4.2.3 of chapter 4. The initial transient occurrence is attributed to wind-diesel mode of operation at start of the simulation. Still it can be observed that the performance of the speed controller is good in tracking the reference speed.

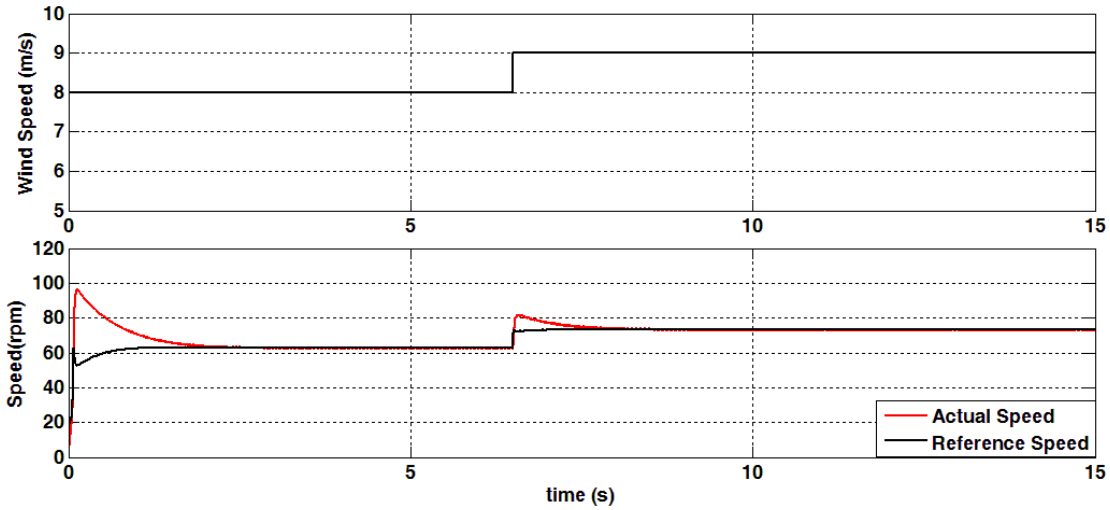

Fig.6. 12. Speed tracking performance for MPPT control scheme

Figure 6.13 depicts the change in operating modes of HWDS: 1) WD mode of operation is shown in simulation time 0 to 7 seconds and 2) WO mode of operation is shown in simulation time 7 to 15 seconds. The transition between modes of operation occurs at 7th second, at this time the diesel generator is shut off and disconnected through a circuit breaker. The transient effect is reflected in the power output of wind turbine. Figure 6.13 also shows the power sharing between the sources and sink in accordance to the wind speed pattern shown in figure 6.12. The detailed discussion of each graph is given below.

Fig.6. 13. Power sharing in different mode of operation in HWDS

The first graph of figure 6.13 shows the wind turbine power output; maximum power extraction from available wind speed can be observed throughout the simulation. Change in wind speed occurs at 6.5 sec, and increased power generation can observed. Power fluctuations observed during simulation time 0 to 7 seconds is attributed to the wind-diesel mode of operation of HWDS, were both the wind turbine and diesel generation system share the power generation required.

Second graph in figure 6.13 shows the diesel generator (DG) power output. The diesel generator is controlled by the governor [66] control system with speed droop adjustment. It can be observed that the diesel generator supplements the wind turbine power output to meet the load demand of 20kW i.e. the DG unit shares the required power generation with wind turbine to supply the load.

The third graph in figure 6.13 shows the load power consumption. The power generated is supplied to the load through smoothening filter reactors. The initial load is 20kW, it can be observed that the load power supplied is shared between sources and excess of is generation is supplied to dump loads to maintain a constant 20kW. At 6.5 seconds an additional 5kW load is added as shown in the graph. Due to the reactors the sharp change (by additional load) in load power is avoided. Throughout the simulation the load is supplied with steady power generation with low fluctuation. Figure 6.14 shows the speed tracking performance of the control system for a different wind speed pattern.

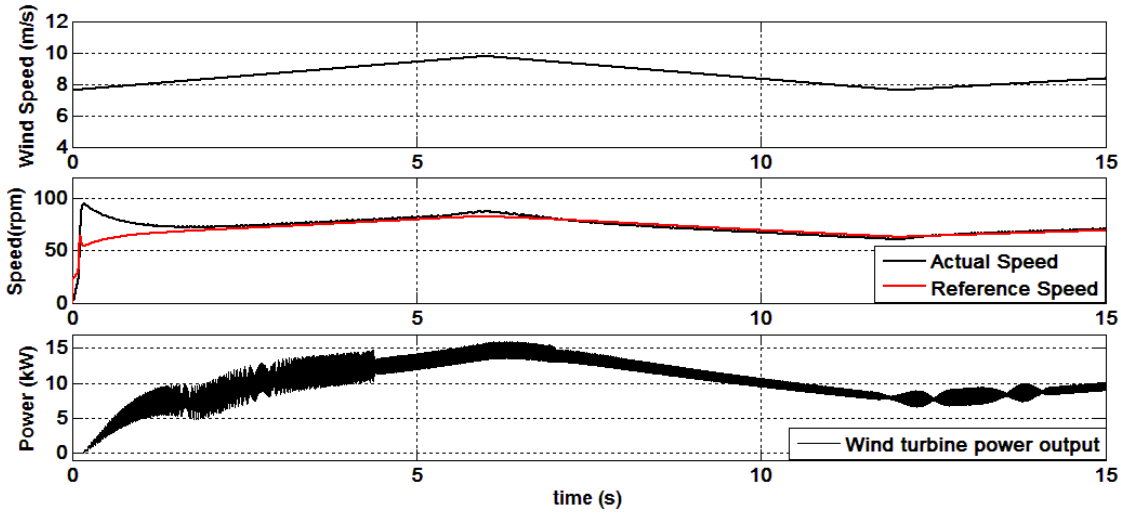

Fig.6. 14. Speed Tracking Performance for Variable Wind Speed

Figure 6.15 shows the regulated power system frequency corresponding to the mode of operation of the HWDS described in figure 6.13. It can be observed that the frequency is regulated at constant 60Hz throughout the simulation.

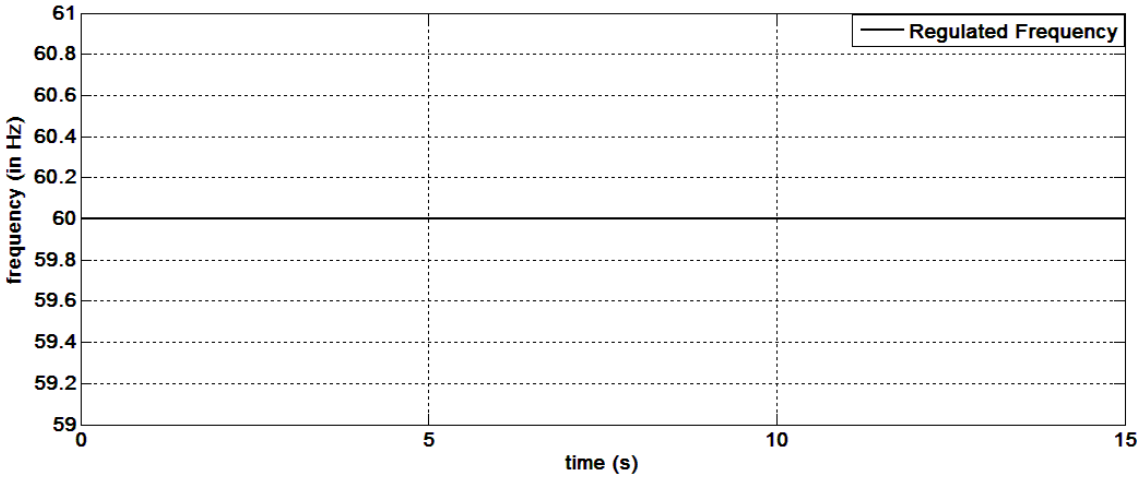

Fig.6. 15. Regulated power system frequency

Figure 6.16 shows the speed tracking performance of the control system under a random step change in the wind speed. It can be observed that the generator rotor speed is controlled to track the random step change in the MPPT reference speed. The transient observed in the beginning of the simulation is mainly attributed to the chosen initial values of power and speed in the MPPT algorithm discussed in section 4.2.2 of chapter 4.

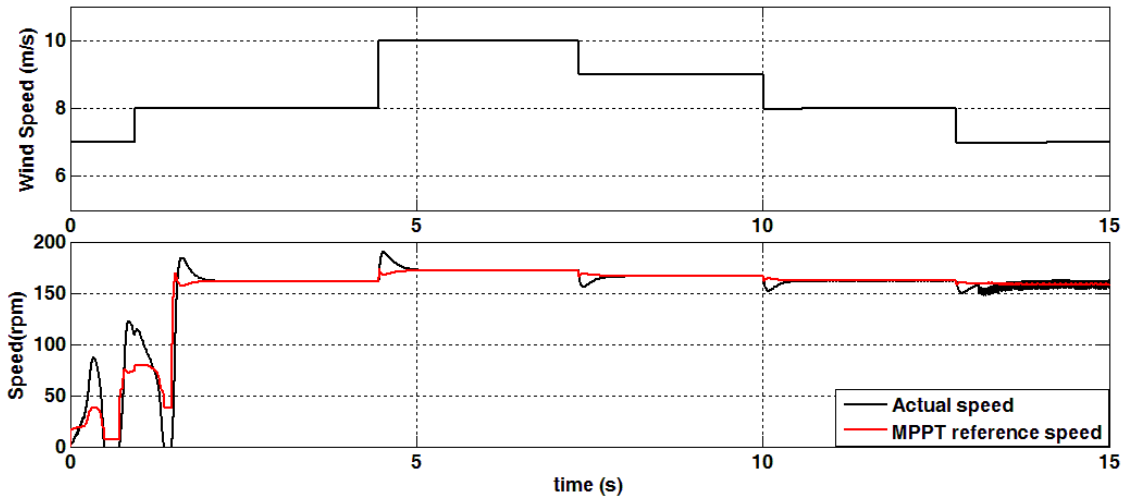

Fig.6. 16. Speed tracking performance under random step change in wind speed pattern

6.3.2. Hybrid Wind Diesel System Based Micro-Grid with DFIG based WECS

Validating the performance of the control system discussed (in section 5.3.2 of chapter 5) for the HWDS is shown by the simulation study results. Figure 6.17 shows the hybrid wind diesel system behaviour during the grid connected mode and isolated mode of operation. In figure 6.17, grid connected mode of operation is shown during simulation time 0 to 3 seconds and 10 to 20 seconds. Similarly isolated wind diesel operation is shown during simulation time 3 to 10 sec.

The graphs in figure 6.17 represent the following: 1) first graph shows the step change (occurring at eighth second) in wind speed, 2) second graph shows the speed tracking, were the reference speed is generated using the MPPT algorithm discussed in section 4.2.3 of chapter 4. At time zero it can be observed that the speed is 150rad/sec, this is the initial speed error due the impact of grid connection [74]. And the speed controller overcomes this impact and tracks the reference speed, 3) third graph shows the wind turbine power output, it can be observed that the power generation reflects the effect of changing rotor speed. In accordance with available wind speed, maximum power extraction can be observed throughout the simulation time. The transient observed at tenth second is attributed to the grid connection, 4) fourth graph shows the load power consumption, initial load is 9MW and an additional load of 5MW is added at fifteenth second, steady load power consumption is observed throughout simulation. The transient observed at tenth second is attributed to changing mode of operation from isolated wind diesel mode to grid connected mode, 5) fifth graph shows the diesel generator output, the

diesel generator connected to the micro-grid through a circuit breaker and it is operated during time 3 to 10 seconds, were the grid supply is disconnected throughout its operation. Between time 0 to 3 seconds and 10 to 20 seconds the diesel generator supply is shut down and disconnected.

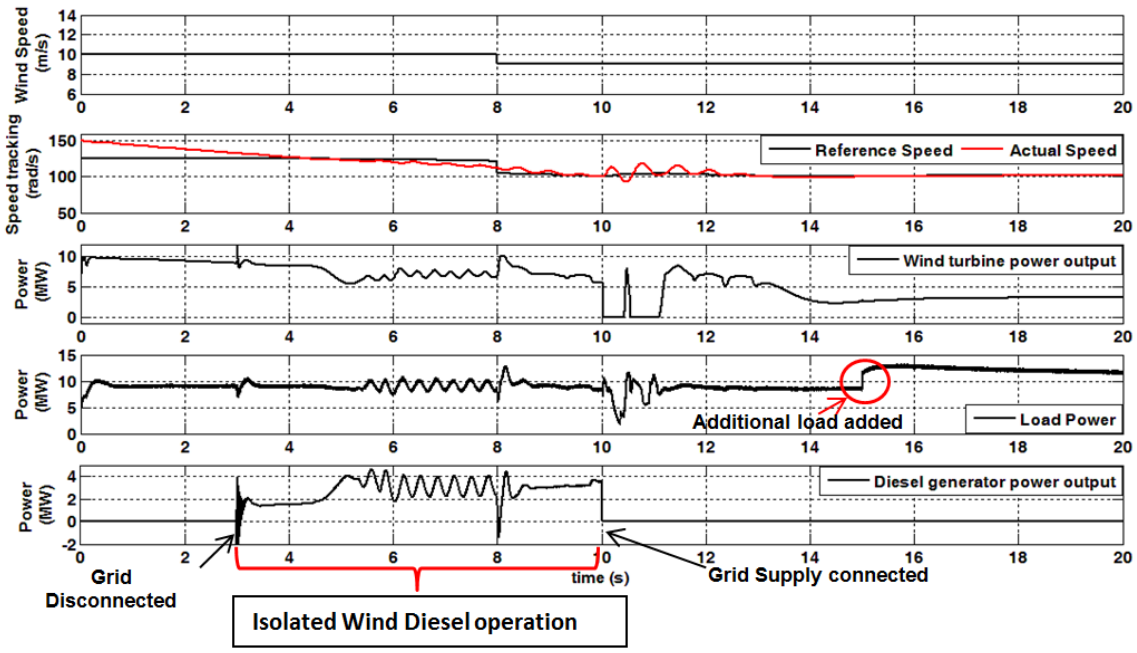

Fig.6. 17. Speed tracking and power sharing in different modes of operation in HWDS

Figure 6.18 shows the DC-link voltage regulator performance corresponding with mode of operation shown in figure 6.17. The voltage regulator regulates the DC-link voltage between the rotor side and grid side converters. It can be observed that the DC-link voltage is regulated at approximately around 1150 volts throughout the simulation except at time 10 to 11 seconds. At 10th second a transient voltage peak is observed, it fluctuates between 500 to 5500 volts for one second approximately, this transient

behavior is attributed to the change in the mode of operation from isolated wind-diesel mode to wind-only mode.

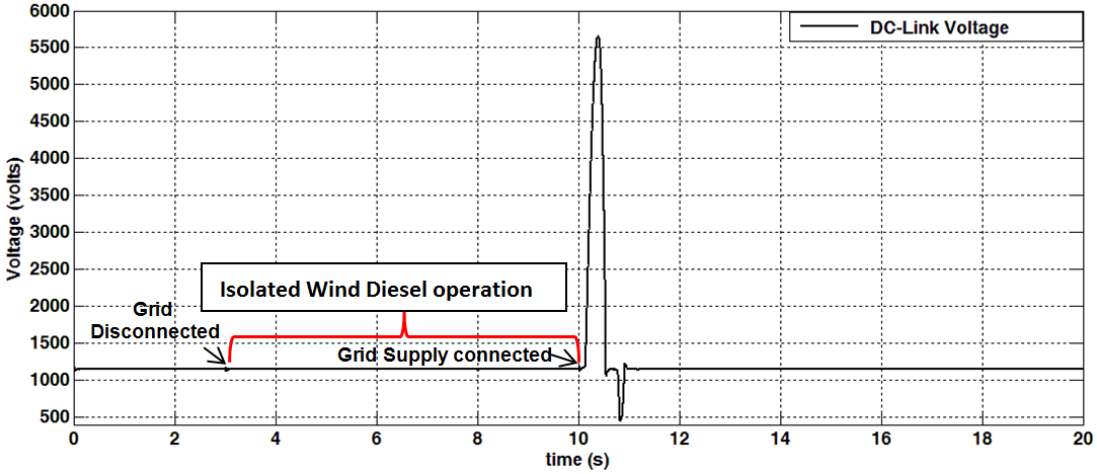

Fig.6. 18. Performance of DC-link voltage regulation system

6.4. Conclusion

Hybrid wind diesel system (HWDS) is an economic reality to reduce the dependency on diesel for powering off-grid communities around the world. However, a complex control system design is required to ensure proper power sharing between the two sources and maintain optimum power quality to meet the power demand. Since the HWDS can be operated as stand-alone and grid connected power system, the control system design for this application is more challenging. Development of control systems for HWDS through simulation study is focused in this thesis. The main contributions of this research work are summarized below.

- Simulation models of hybrid wind diesel system (HWDS) based stand-alone system and micro-grid system is developed with different types of generator for fully-rated converter based wind energy conversion system

- A multi-variable control system is developed and implemented into the simulation models of HWDS. This control system achieves the following: a) ensures power sharing and maintains power balance consistency between sources and sinks (i.e. loads), b) regulates the power quality at optimum level, and c) extracts the maximum power from available wind
- An improved maximum power point tracking control scheme for wind turbine system is implemented into the simulation models
- Performance of the developed control system is validated by simulating the transitions between different modes of operation of HWDS. The results obtained in this validation is presented and discussed

6.5. Suggestions for Future Work

The overall performance of the control strategy developed in this work can be improved by including advanced control techniques like fuzzy logic, sliding mode control etc. A control strategy for smooth transition between different HWDS operating modes discussed in [12] can be included for improved system performance. Addition of sources like storage unit, solar photovoltaic etc. to the hybrid system will increase the reliability

of the system. Further a more realistic wind pattern can be used in the future work involving simulation study.

Appendix A. Specifications of the System Used in Simulation Study

A.1. Stand-Alone HWDS with PMSG Based WECS

Wind turbine parameters*:* c_1 = 0.5176, c_2 = 116, c_3 = 0.4, c_4 = 5, c_5 = 21 and c_6 = 0.0068, ρ = 1.225 kg/m^3, Rotor swept area=107.5m^2

Permanent Magnet Synchronous Generator (used in WECS): Nominal power = 30kW, R_s= 0.05, L_d = 0.000635, L_q =0.000635, frequency=60Hz

Synchronous Generator (used in diesel generation system): Nominal power =52.5kW, frequency=60Hz, R_s = 0.003 Pu, H= 0.1349 pu, F = 0.02098, pole pairs = 2

A.2. Hybrid Wind Diesel System Based Micro-Grid

Wind turbine parameters*:* c_1 = 0.5176, c_2 = 116, c_3 = 0.4, c_4 = 5, c_5 = 21 and c_6 = 0.0068, ρ = 1.225 kg/m^{3,} Rotor diameter = 82.5m

Double-fed induction generator (used in WECS): Nominal Power = 1.5MW, frequency=60Hz, R_s= 0.023 pu, L_s =0.18 pu, R'_r = 0.016 pu, L'_r= 0.16 pu, L_m=2.9 pu

Synchronous Generator (used in diesel generation system): Nominal power =3.125MW, frequency=60Hz, R_s = 0.0036 pu, H= 1.07 pu, pole pairs = 2

A.3. Squirrel-Cage Induction Generator Based Stand-Alone WECS

Wind turbine parameters*:* c_1 = 0.5176, c_2 = 116, c_3 = 0.4, c_4 = 5, c_5 = 21 and c_6 = 0.0068, ρ = 1.225 kg/m^3

Squirrel-Cage Induction machine (used in WECS): Nominal power = 30kW, R_S =0.087 Ohms, L_s= 0.8e-3 H, R'_r= 0.228 Ohms, L'_r 0.8e-3 H and L_m= 34.7e-3 H

A.4. Electrical Grid System

Three-phase voltage source (positive sequence parameters): RMS voltage (phase-phase) = 120KV, Phase = 0 degree, frequency = 60HZ

Three-phase impedance: Positive sequence parameters – R1=0.5760 Ohms, L1= 0.0153 H, zero sequence parameters – R 0=1.728 Ohms, L0= 0.0458 H

Three-phase transformer (120KV/25KV): Nominal power=47e6 VA, frequency=60, winding 1 parameters – V1 rms (phase-phase) = 120e3V, R1=0.00266 pu, L1=0.08 pu, Winding 2 parameters – V2 rms (phase-phase) = 25e3, R2=0.00266pu, L2=0.08pu

Three-phase transmission line (pi section model): Frequency =60 HZ, Positive sequence parameters – resistance r1=0.1153 ohms/km, inductance L1=1.05e-3 H/km, capacitance C1=11.33e-009 F/km, Zero sequence parameters – resistance r1=0.413 ohms/km, inductance L1=3.32e-3 H/km, capacitance C1=5.01e-009 F/km, Line length = 30km

Three-phase transformer (25KV/575V): Nominal power=10.5e6 VA, frequency=60, winding 1 parameters – V1 rms (phase-phase) = 25e3V, R1=8.3333e-04 pu, L1=0.025 pu, Winding 2 parameters – V2 rms (phase-phase) = 575V, R2=8.3333e-04, L2=0.025pu

References

[1] Government of Canada Publications, "Status of Remote/Off-Grid Communities in Canada," August 2011. [Online]. Available: http://publications.gc.ca/collections/collection_2013/rncan-nrcan/M154-71-2013-eng.pdf.

[2] K. Ah-You, G. Leng, "Renewable energy in Canada's remote communities," in *Renewable energy for remote communities program natural resources Canada*, 1997.

[3] V. Singh, "Blending wind and solar into the diesel generator market," Renewable enegy policy project- Research report, 2001.

[4] Wind Energy TechnoCentre, [Online]. Available: https://www.eolien.qc.ca/en/.

[5] *WIND ENERGY THE FACTS: An analysis of wind energy in EU-25,* European Wind Energy Association (EWEA), 2002.

[6] I. Baring-Gould and M. Dabo, "Technology, Performance, and Market Report of Wind-Diesel Applications for Remote and Island Communities," in *WINDPOWER 2009 Conference and Exhibition*, Chicago, Illinois, May 2009.

[7] T. S. Bhatti, A. A. F. Al-Ademi, N. K. Bansal, "Dynamics and control of isolated wind-diesel power systems," *International Journal of Energy Research*, vol. 19, no. 8, p. 729–740, 1995.

[8] Wind-Diesel Systems Architecture Guidebook, American Wind Energy Association, 1991.

[9] S. A. Papathanassiou, M. P. Papadopoulos, "Dynamic characteristics of autonomous wind–diesel systems," *Renewable Energy,* vol. 23, no. 2, p. 293–311, 2001.

[10] E. Muljadi , H.E. McKenna, "Power quality issues in a hybrid power system," *Power quality issues in a hybrid power system,* vol. 38, no. 3, pp. 803 - 809, 2002.

[11] R. Sebastia´n, R. Pen˜a Alzola, "Effective active power control of a high penetration wind diesel system with a Ni–Cd battery energy storage," *Renewable Energy,* vol. 35, no. 5, p. 952–965, 2010.

[12] R. Sebastián, "Smooth transition from wind only to wind diesel mode in an autonomous wind diesel system with a battery-based energy storage system," *Renewable Energy,* vol. 33, no. 3,

p. 454–466, 2008.

[13] R. Sebastian, "Modelling and simulation of a high penetration wind diesel system with battery energy storage," *International Journal of Electrical Power & Energy Systems,* vol. 33, no. 3, p. 767–774, 2011.

[14] H. Sharma,S. Islam, Pryor, "Dynamic modeling and simulation of a hybrid wind diesel remote area power system," *International Journal of Renewable Energy Engineering,* vol. 2, no. 1, pp. 19-25, 2000.

[15] S.A. Lone, M.Mufti, "Power quality improvement of a stand-alone power system subjected to various disturbances," *Journal of Power Sources,* vol. 163, no. 1, p. 604–615, 2006.

[16] A.M.O. Haruni, A. Gargoom, M.E. Haque, M.Negnevitsky, "Voltage and frequency stabilisation of wind-diesel hybrid remote area power systems," in *Power Engineering Conference, 2009. AUPEC 2009. Australasian Universities*, Adelaide, SA, 2009.

[17] A. M. Kassem, A. M. Yousef, "Robust control of an isolated hybrid wind–diesel power system using Linear Quadratic Gaussian approach," *International Journal of Electrical Power & Energy Systems,* vol. 33, no. 4, p. 1092–1100, 2011.

[18] R. Hunter, G. Elliot, Wind-Diesel Systems: A Guide to the Technology and Its Implementation, Cambridge University Press, 1994.

[19] B. Sedaghat , A. Jalilvand, R. Noroozian, "Design of a multilevel control strategy for integration of stand-alone wind/diesel system," *International Journal of Electrical Power & Energy Systems,* vol. 35, no. 1, p. 123–137, 2012.

[20] A.M.O. Haruni, A.M.O, A. Gargoom, M.E. Haque, M. Negnevitsky, "Dynamic operation and control of a hybrid wind-diesel stand alone power systems," in *Applied Power Electronics Conference and Exposition (APEC), 2010 Twenty-Fifth Annual IEEE*, Palm Springs, CA, 2010.

[21] J.M. Rodrigues, F.O. Resende, C.L. Moreira, "Contribution of PMSG based small wind generation systems to provide voltage control in low voltage networks," in *Innovative Smart Grid Technologies (ISGT Europe), 2011 2nd IEEE PES International Conference and Exhibition*, Manchester, 2011.

[22] N. Mendis, K.M. Muttaqi, S. Sayeef, S. Perera, "Standalone Operation of Wind Turbine-Based Variable Speed Generators With Maximum Power Extraction Capability," *Energy Conversion, IEEE Transactions,* vol. 27, no. 4, pp. 822 - 834, 2012.

[23] A. Gupta, D.K. Jain, D.K, S. Dahiya, "Hybrid operation of diesel generator with WECS using back to back converters and BESS," in *Power India Conference, 2012 IEEE Fifth*, Murthal, 2012.

[24] A. Arulampalam, N. Mithulananthan,R.C. Bansal, T.K. Saha, "Micro-grid control of PV-Wind-Diesel hybrid system with islanded and grid connected operations," in *Sustainable Energy Technologies (ICSET), 2010 IEEE International Conference*, Kandy, 2010.

[25] K.S. Jeon, J.H.Cho, C.H. Hee; A. Jong-Bo, W.H. Sae-Hyuk, "Dynamic Modeling and Control of a Grid-Connected Hybrid Generation System With Versatile Power Transfer," in *Industrial Electronics, IEEE Transactions*, 2008.

[26] W. Haining, N. Chemmangot V, S. Jianhui,D. Ming, "Control and Interfacing of a Grid-Connected Small-Scale Wind Turbine Generator," *Energy Conversion, IEEE Transactions*, vol. 26, no. 2, pp. 428 - 434, 2011.

[27] C.Cristea,J.P.Lopes, M.Eremia, L.Toma, "The control of isolated power systems with wind generation," in *Power Tech, 2007 IEEE Lausanne* , Lausanne , 2007.

[28] M. M. T. Ansari, S. Velusami, "DMLHFLC (Dual mode linguistic hedge fuzzy logic controller) for an isolated windediesel hybrid power system with BES (battery energy storage) unit," *Energy, Elsevier*, vol. 35, no. 9, pp. 3827-3837, 2010.

[29] E.Kamal, M.Koutb, A.A.Sobaih, S.Kaddah, "Maximum Power Control of Hybrid Wind-Diesel-Storage System," *Advances in Fuzzy Systems*, vol. 2008, p. 9, 2008.

[30] Y. Hu, Z. Chen, "Modeling of Frequency and Power Control in An Autonomous Power System with Wind Turbines and Diesel Generation Units," in *Transmission and Distribution Conference and Exhibition: Asia and Pacific, 2005 IEEE/PES* , Dalian, 2005.

[31] P. Sivakumar, S. Thirukkovai, K. Yogeshraj, A. Abdullah, "Reactive Power Regulation of Wind-Diesel Hybrid System," in *INTERNATIONAL CONFERENCE ON MODELLING OPTIMIZATION AND COMPUTING*, Kumarakoil, Kanyakumari District, 2012.

[32] R. Sebastián, "Reverse power management in a wind diesel system with a battery energy storage," *International Journal of Electrical Power & Energy Systems*, vol. 44, no. 1, p. 160–167, 2013.

[33] CM.Hong,TC.Ou, KH.Lu, "Development of intelligent MPPT (maximum power point tracking) control for a grid-connected hybrid power generation system," *Energy, Elsevier*, vol. 50, p. 270–279, 2013.

[34] V. FRIEDEL, *MODELING AND SIMULATION OF A HYBRID WIND-DIESEL MICROGRID*, Stockholm, Sweden: KTH School of Electrical Engineering, 2009.

[35] V. Rajasekaran, A.Merabet, H.Ibrahim, R.Beguenane,J.Thongam, "Maximum power point tracking and frequency control for hybrid wind diesel system supplying an isolated load," in *IECON 2012 - 38th Annual Conference on IEEE Industrial Electronics Society* , Montreal, QC, 2012.

[36] V. Rajasekaran, A.Merabet, H.Ibrahim, R.Beguenane,J.S.Thongam, "Control System Simulation for Stand-Alone Hybrid Wind Diesel System," in *Electrical Power and Energy Conference (EPEC), 2013 IEEE* , Halifax, NS, 2013.

[37] V. Rajasekaran, A.Merabet, H.Ibrahim, R.Beguenane,J.S.Thongam, "Control System for Hybrid Wind Diesel Based Microgrid," in *Electrical Power and Energy Conference (EPEC), 2013 IEEE*, Halifax, NS, 2013.

[38] R. W. Righter, Wind Energy in America: A History, University of Oklahoma Press, 1996.

[39] A.M. Bobely and J. F. Kreider, Distributed Generation: The Power Paradigm for the New Millennium, CRC Press LLC, 2001.

[40] M. Jaccard, "Renewable Portfolio Standard," *Encyclopedia of Energy, Elsevier,* vol. 5, pp. 413-421, 2004.

[41] T. Ackermann, Wind Power in Power Systems, Wiley, 2005.

[42] "Canadian Wind Energy Association (canWEA)," [Online]. Available: http://www.canwea.ca/.

[43] S. Mathew, Wind Energy: Fundamentals, Resource Analysis and Economics, Netherlands: Springer, 2006.

[44] Office of Energy Efficiency and Renewable, "Energy Efficiency and Renewable Energy," U.S. Department of Energy, [Online]. Available: http://www1.eere.energy.gov/windandhydro/images/illust_large_turbine.gif, http://www1.eere.energy.gov/windandhydro/wind_how.html.

[45] N. Mohan, T. Undeland, and W. Robbins, Power Electronics: Converters, Applications, and Design, Third ed., Wiley, 2009.

[46] F. Blaabjerg, Z. Chen, R. Teodorescu, F. Iov, "Power Electronics in Wind Turbine Systems," in *Power Electronics and Motion Control Conference, 2006. IPEMC 2006. CES/IEEE 5th*

International, Shanghai, 2006.

[47] F. Blaabjerg, Z. Chen, Power Electronics for Modern Wind Turbines, Morgan & Clay-pool Publishers, 2006.

[48] B. Wu, Y.Lang, N. Zargari, S.Kouro, Power Conversion and Control of Wind Energy Systems, New Jersey: Wiley-IEEE Press, 2011.

[49] D.J. Burnham, S. Santoso, E. Muljadi, "Variable rotor-resistance control of wind turbine generators," in *Power & Energy Society General Meeting, 2009. PES '09. IEEE*, Calgary, AB, 2009.

[50] S. Li, S. Sinha, "A simulation analysis of double-fed induction generator for wind energy conversion using PSpice," in *Power Engineering Society General Meeting, 2006. IEEE*, Montreal, Quebec, 2006.

[51] I. Boldea, The Electric Generators Handbook: Variable Speed Generators, CRC Press, Taylor & Francis group, 2006.

[52] J.M. Carrasco, L.G.Franquelo, J.Bialasiewicz, E. Galvan, R. Guisado, M. Prats, J. Leon and N. Moreno-Alfonso, "Power-Electronic Systems for the Grid Integration of Renwable Energy Sources: A Survey," *IEEE Transactions on Industrial Electronics*, pp. 1002-1016, 2006.

[53] "Electrical know how, Classification of electric motors - part two," [Online]. Available: http://www.electrical-knowhow.com/2012/05/classification-of-electric-motors-part.html.

[54] "Mathworks Documentation Center, Simpowersystems," MathWorks Inc, 2013. [Online]. Available: http://www.mathworks.com/help/physmod/powersys/index.html.

[55] B. Dosijanoski, "Simulation of Doubly-Fed Induction Generator in a Wind Turbine," 17-20 October 2009. [Online]. Available: http://mechatronika.polsl.pl/owd/pdf2009/378.pdf.

[56] G.M. Pellegrino, P.D. Torino, F. Villata, P. Guglielmi, A. Vagati, "Design of direct-drive, low-speed PM machines," in *Industry Applications Conference, 2003. 38th IAS Annual Meeting*, 2003.

[57] F. Blaabjerg, F. Iov,Z.Chen, K. Ma, "Power electronics and controls for wind turbine systems," in *Energy Conference and Exhibition (EnergyCon), 2010 IEEE International*, Manama, 2010.

[58] H. Siegfried, Grid Integration of Wind Energy Conversion Systems, John Wiley & Sons Ltd, 1998.

[59] "http://hotzdev.com," Hotz Development - Renewable Energy, 2013. [Online]. Available: http://hotzdev.com/wp-content/uploads/2011/10/EO2512-Direct-Drive-Wind-Turbine-Hotz-Development.pdf.

[60] M. Zhou,G. Bao, Y. Gong, "Maximum Power Point Tracking Strategy for Direct Driven PMSG," in *Power and Energy Engineering Conference (APPEEC), 2011 Asia-Pacific*, Wuhan, 2011.

[61] J.S. Thongam, P. Bouchard, H. Ezzaidi, "Wind speed sensorless maximum power point tracking control of variable speed wind energy conversion systems," in *Electric Machines and Drives Conference, 2009. IEMDC '09. IEEE International*, Miami, FL, 2009.

[62] A. Merabet, V. Rajasekaran, A. McMullin, H. Ibrahim, R. Beguenane, J.S. Thongam, "Nonlinear model predictive controller with state observer for speed sensorless induction generator–wind turbine systems," *Journal of Systems and Control Engineering,* vol. 227, no. 2, pp. 199-213, 2013.

[63] J. B. Ekanayake, L.Holdsworth, X. Wu, N. Jenkins, "Dynamic Modeling of Doubly Fed Induction Generator Wind Turbines," *IEEE TRANSACTIONS ON POWER SYSTEMS,* pp. 803-809, May 2003.

[64] E. I. Baring-Gould, "National Renwable Energy Laboratory, U.S. Department of Energy," 2009. [Online]. Available: http://apps1.eere.energy.gov/tribalenergy/pdfs/wind_akwd04_basics.pdf.

[65] L.N. Hannett, F.P. Mlello,G.H. Tylinski, W.H. Becker, "Validation of Nuclear Plant Auxiliary Power Supply By Test," *Power Apparatus and Systems, IEEE Transactions,* pp. 3068 - 3074, September 1982.

[66] K.E. Yeager, J.R. Willis, "Modeling of emergency diesel generators in an 800 megawatt nuclear power plant," *Energy Conversion, IEEE Transactions,* pp. 433 - 441, September 1993.

[67] G.S. Stavrakakis, G.N. Kariniotakis, "A general simulation algorithm for the accurate assessment of isolated diesel-wind turbines systems interaction. I. A general multimachine power system model," *Energy Conversion, IEEE Transactions,* pp. 577-583, Sept 1995.

[68] F. Mohamed, "MICROGRID MODELLING AND SIMULATION," Helsinki University of Technology, Finland, 2006.

[69] S. Roy, O.P. Malik, G.S. Hope, "An adaptive control scheme for speed control of diesel driven power-plants," *Energy Conversion, IEEE Transactions,* pp. 605 - 611, Dec 1991.

[70] "IEEE Recommended Practice for Excitation System Models for Power System Stability Studies," IEEE Power Engineering Society, New York, NY, IEEE Std 421.5™-2005 (Revision of IEEE Std 421.5-1992).

[71] R. Sebastián, R. Peña Alzola, "Simulation of an isolated Wind Diesel System with battery energy storage," *Electric Power Systems Research*, vol. 81, no. 2, p. 677–686, 2011.

[72] N. Mendis, K.M Muttaqi, S.Sayeef, S. Perera, S., "A control approach for voltage and frequency regulation of a Wind-Diesel-battery based hybrid remote area power supply system," in *IECON 2010 - 36th Annual Conference on IEEE Industrial Electronics Society*, Glendale, AZ, 2010.

[73] A. S. David, "Generator Basics Applied to Field Problems," *NETA WORLD MAGAZINE*, Summer 1993.

[74] F. Mei, B. Pal, "Modal Analysis of Grid-Connected Doubly Fed Induction Generators," *Energy Conversion, IEEE Transactions*, vol. 22, no. 3, pp. 728 - 736, 2007.

[75] P. Lundsager, H. Bindner, "A Simple, Robust, and Reliable Wind-Diesel Concept for Remote Power Supply," *Renewable Energy*, vol. 5, no. 1-4, p. 626–630, 1994.

[76] S. Jöckel, A. Herrmann, J. Rinck, "High Energy Production plus Built-in Reliability – the New VENSYS 70 / 77 Gearless Wind Turbines in the 1.5 MW Class," in *European Wind Energy Conference and Exhibition, EWEC*, 2006.